FACULDADE DE ENGENHARIA DA UNIVERSIDADE DO PORTO

Operational Analysis of Distribution Systems Featuring Large-scale Variable RES: Contributions of Energy Storage Systems and Switchable Capacitor Banks

Mário Pascoal Santos Pereira

Dissertação realizada no âmbito do
Mestrado Integrado de Engenharia Eletrotécnica e de Computadores
Major Energia

Orientador: Prof. Doutor João Paulo da Silva Catalão

Co-orientador: Doutor Desta Zahlay Fitiwi

Julho de 2017

Resumo

Na última década, o nível de fontes de energia renovável (RESs) de cariz variável, integradas no sistema de distribuição, tem vindo a aumentar continuamente. Este aumento gera mais incerteza nos sistemas, que já contêm diversas fontes tradicionais de incerteza, e outras que dizem respeito a tecnologias emergentes relacionadas com resposta à procura e com veículos elétricos. Por conseguinte, os operadores do sistema de distribuição enfrentam maiores dificuldades em manter a operação ótima destes sistemas.

É expectável que estes desafios/limitações sejam ultrapassados através de uma transformação da rede atual para uma inteligente (*smart grid*), equipada com os sistemas de armazenamento de energia (ESSs) e bancos variáveis de condensadores (SCBs). Estas tecnologias proporcionam maior flexibilidade, permitindo uma operação mais eficiente na presença de acrescida incerteza e variabilidade, características inerentes à maioria das RESs (por exemplo: produção eólica e solar).

A presente dissertação propõe um modelo de programação estocástica linear inteira-mista, cujo objetivo é otimizar a operação de sistemas de distribuição, com elevada integração de RES de cariz variável, recorrendo a tecnologias de ESSs e a SCBs, de forma a aliviar os impactos negativos de fontes renováveis na performance do sistema elétrico. A otimização baseia-se num modelo de rede de corrente alternada linearizado. Além disso, o modelo de operação proposto é formulado tendo em conta tanto a variabilidade como a incerteza, que são características comuns à procura e à produção eólica e solar. Tendo em conta estas considerações, é possível realizar uma análise mais realista, sob diversas condições de operação. A função objetivo do modelo proposto é minimizar a soma dos custos esperados, nomeadamente a soma dos custos de operação do sistema, de potência não fornecida e de emissões, ainda assim respeitando limites técnicos e económicos.

A análise de resultados cobre diversos temas, mas sempre na perspetiva de maximizar a integração de energia de fontes renováveis, sem prejudicar a estabilidade e integridade do sistema bem como a qualidade da energia entregue aos clientes. Nesse sentido, a dissertação apresenta uma análise extensiva relativa aos impactos de SCBs e ESSs de eficiências diferentes (quer em conjunto, quer individualmente) no sistema. Em particular, em termos de custos, perdas, tensões e mix de energia, a performance do sistema foi analisada pormenorizadamente, representando uma das principais contribuições desta dissertação. Os resultados das simulações indicam que ESSs e SCBs estrategicamente colocados podem aumentar o nível de utilização de potência com origem em RES e, simultaneamente, amortizar os impactos negativos da intermitência destas fontes no sistema considerado. Por exemplo, as perdas da rede são reduzidas em mais de 70% e os custos totais do sistema em 69%. Para além disso, a presença de ESSs e SCBs permite alcançar quotas de 96.1% de RESs no mix de energia. Consequentemente, a energia importada da rede a montante representa apenas 3.9%, o que significa que o sistema opera em modo ilha a maior parte do tempo, num período de 24 horas. Desta forma, os sistemas de distribuição poderão atingir a ausência de emissões de carbono respondendo à procura através de produção local mais "limpa".

Palavras-chave - Análise operacional, bancos variáveis de condensadores, incerteza RES, operação ótima, programação estocástica, programação linear inteira-mista, sistemas de armazenamento de energia, sistemas de distribuição

Abstract

In the last decade, the level of variable renewable energy sources (RESs) integrated in distribution network systems have been continuously growing. This adds more uncertainty to these systems, which also face many traditional sources of uncertainty, and those pertaining to other emerging technologies such as demand response and electric vehicles. As a result, distribution system operators are finding it increasingly difficult to maintain an optimal operation of such network systems.

These challenges/limitations are, however, expected to be alleviated when distribution systems undergo the transformation process to smart grids, equipped with appropriate technologies such as energy storage systems (ESSs) and switchable capacitor banks (SCBs). These technologies offer more flexibility in the system, allowing effective management of the uncertainty and variability pertaining to most RESs (such as wind and solar PV power sources).

This dissertation presents a stochastic mixed integer linear programming (SMILP) model, aiming to optimally operate distribution network systems, featuring large-scale variable renewables, and alleviate the negative impacts of RESs on the overall performance of such systems by means of ESSs and SCBs. The optimization model is based on a linearized AC network model. Furthermore, the proposed operational model is formulated in a stochastic environment, particularly accounting for both variability and uncertainty pertaining to demand, wind and solar power productions. Such considerations allow one to make a more realistic analysis, under various operational conditions. The objective function of the proposed model is to minimize the sum of expected costs of operation, unserved power and emissions while meeting the most relevant technical and economic constraints.

The analysis covers several issues, but with the perspective of maximizing the utilization level of variable RESs, and most importantly, without endangering the stability and integrity of the system as well as the quality of power delivered to the consumers. In this line, the dissertation presents an extensive analysis concerning the impacts of SCBs and ESSs of different efficiencies (either collectively or individually) in the system. In particular, the overall system performance in terms of costs, losses, voltages and energy mix has been extensively analysed, which is one of the main contributions of this dissertation. Simulation results indicate that strategically placed ESSs and SCBs can substantially increase the usage level of RES power, and simultaneously alleviate the negative impacts of RES intermittency in the considered system. For example, network losses are slashed by more than 70% and total system costs by 69%. Furthermore, the presence of ESSs and SCBs leads to as high as 96.1% share of RESs in the overall energy mix in the considered system. The energy imported through the substation in this case is limited to 3.9%, which means that the system operates in island mode for most of the time during the 24-hour period. This means that distribution network systems can go "carbon-free" by meeting a large portion of the demand using "cleaner" power locally produced.

Key Words - Distribution systems, energy storage systems, mixed integer linear programming, operational analysis, optimal operation, RES uncertainty, stochastic programming, switchable capacitor banks

Acknowledgments

I would like to express my gratitude to my supervisor Professor João Catalão for accepting me under his supervision and allowing me the opportunity to work in such interesting subject.

I would also like to thank Doctor Desta Fitiwi and Sérgio Santos, for being available for all the questions that have emerged along the way, and for their vital advices.

Finally, I must express my very profound gratitude to my family and my friends for providing me with the support and continuous encouragement throughout my years of study.

Thank you all.

Mário Pereira

"...man, in his quest for knowledge and progress,
is determined and cannot be deterred."

John F. Kennedy

Contents

List of Figures

List of Tables

Abbreviation and Symbols

List of Abbreviations

DFIG	Doubly feed induction generator
DG	Dispersed Generation
EFF	Efficiency
ESS	Energy storage system
EU	European Union
MILP	Mixed integer linear programming
MISOCP	Mixed-integer second order programming
PV	Photovoltaic
RES	Renewable energy systems
SCB	Switchable Capacitor Bank
SMILP	Stochastic mixed integer linear programming

List of Symbols

Set/Indices	
i/Ω^{i}	Index/set of buses
$g/\Omega^{g}/\Omega^{DG}$	Index/set of generators/DGs
l/Ω^{l}	Index/set of branches
s/Ω^{s}	Index/set of scenarios
h/Ω^{h}	Index/set of hours
cb/Ω^{cb}	Index/set of capacitor banks
ζ/Ω^{ζ}	Index/set of substations
$c(i)$	Index for CB blocks at node i
y	Index of linear segments

Parameters	
$E_{es,i}^{min}$, $E_{es,i}^{max}$	Energy storage limits (MWh)
ER_g, ER_{SS}	Emission Rates of DGs and energy purchase upstream, respectively (tCO_2e/MWh)
g_l, b_l, S_l^{max}	Conductance, susceptance and flow limit of branch l, respectively (℧, ℧, MVA)
$OC_{g,i,s,h}$	Operation cost of DGs (€/MWh)
P_l^{max}, Q_l^{max}	Limits of active and reactive flows on branch l (MW, MVAr)
pf_g	DG power factor
pf_{ss}	Power factor of substation
$Q_i^{cb,\,max}$	Maximum capacitor bank capacity installed at node i
r_l, x_l	Resistance and Reactance of branch l, respectively

$u_{es,i,h}$	Utilization status of storage system (1 if connected, 0 if disconnected)
V_{nom}	Nominal voltage (kV)
$v^P_{s,h}$, $v^Q_{s,h}$	Penalty for unserved active and reactive power, respectively (€/MW, €/MVAr)
Y, y	Total number of linear segments, index of linear segments
$\alpha_{l,y}$, $\beta_{l,y}$	Slopes of linear segments y on branch l
η^{ch}_{es}, η^{dch}_{es}	Charging and discharging efficiencies of storage systems (%)
δ_1, δ_2, δ_3	Weights
ΔV^{min}, ΔV^{max}	Limits for voltage deviations (kV)
$\lambda^{\zeta}_{s,h}$	Price of electricity purchase from upstream (€/MWh)
$\lambda^{CO2}_{s,h}$	Price of emissions (€/tCO_2e)
ρ_{dem}	Probability of demand scenario *dem*
ρ_s	Probability of scenario s
ρ_{sol}	Probability of solar power production scenario *sol*
ρ_{win}	Probability of wind power production scenario *win*

Variables

$DemP^i_{s,h}$, $DemQ^i_{s,h}$	Active and reactive power demand t node i (MW, MVAr)
$E_{es,i,s,h}$	Stored energy (MWh)
$I^{ch}_{es,i,h}$, $I^{ch}_{es,i,h}$	Charge and discharge indicator variable
$P^{SS}_{\zeta,s,h}$, $Q^{SS}_{\zeta,s,h}$	Active and reactive power import from grid (MW, MVAr)
$P^{ch}_{es,i,s,h}$, $P^{dch}_{es,i,s,h}$	Charged and discharged power from storage system (MW)
$P_{g,i,s,h}$	Active power produced by DGs (MW)
$P^{un}_{i,s,h}$, $Q^{un}_{i,s,h}$	Active and reactive power unserved ant node i (MW, MVAr)
$p_{l,s,h,y}, q_{l,s,h,y}$	Steps used to linearize the quadratic flows (MW, MVAr)
$P_{l,s,h}$, $Q_{l,s,h}$, $\theta_{l,s,h}$	Active and reactive power flows, and voltage angle difference of branch l, respectively (MW, MVAr, radians)
$PL_{l,s,h}$, $QL_{l,s,h}$	Active and reactive power losses (MW, MVAr)
$Q_{g,i,s,h}$	Active power produced/consumed by DGs (MVAr)
$Q^{cb}_{i,s,h}$	Reactive power injected at node i by capacitor bank (MVAr)
$X_c(i,s,h,c(i))$	Binary variable to model CB blocks
$V_{i,s,h}$, $V_{j,s,h}$	Voltage magnitudes of node i and j where both nodes belong to the same branch (kV)
$\theta_{i,s,h}$, $\theta_{j,s,h}$	Voltage angles at node i and j where both nodes belong to the same branch (radians)
$\lambda^{dch}_{s,h}$	Price of electricity discharged from storage system (€/MWh)

Chapter 1

Introduction

This chapter provides a brief introduction, describes the problem addressed and outlines the main motivations and objectives of the research work. In addition, it presents the research methodology and the overall organization of this dissertation.

1.1 Background

In order to reduce the heavy dependence on fossil fuels for energy consumption and emissions as well as tackle the dire consequences of environmental change, renewable energy sources are considered a promising solution. For example, in the European Union there is a target put in place to increase the share of renewable energy in gross final consumption to 20% by 2020. In fact, one of the main concerns in the European Union's energy strategy in the past ten years has been to implement a number of different policies in order to incentivise the production of electricity from renewable sources. This effort has been effective in promoting the integration of such sources, both in short and long term, as the share of renewables is increasing and so is its installed capacity [1].

One of the main challenges regarding renewable energy sources (RESs) integration into power systems is the inherent uncertainty and variability. In fact, unlike conventional power production systems RESs, especially wind and solar power production are completely dependent on weather conditions, which are also increasingly variable due to climate change. Furthermore, the large scale implementation of such systems introduces a number of technical problems such as voltage rise issues, power flow uncertainty, amongst others. Such challenges need to be overcome if the system is to integrate RES in large scales. Therefore, the distribution grid needs to be reshaped in order to accommodate this emerging technology [2].

Energy storage systems (ESSs) offer an interesting technological solution to compensate the stochastic nature of RES power outputs, without having to depend on fossil fuel based production for backup [3]. Since power production from RESs, such as solar PV and wind, is highly variable and uncertain, ESSs can provide a bridge between demand and RESs, by supplying power in low production periods and storing excess power during high production ones.

Capacitor banks are devices widely used for their efficiency in reactive power compensation, and when optimally installed in distribution systems, they provide additional benefits such as loss reduction and voltage control [4], [5]. However, traditionally, distributed reactive power sources were installed as fixed capacitor banks. The inclusion of switchable capacitor banks (SCBs) allow the distribution system operator to have a more flexible control of the system's voltage, power factor and losses.

However, to integrate such technologies in the distribution system and manage their overall complexity, it is necessary to implement new grid concepts such as Smart-grid and Micro-grid, which allow the operator to have access to more information regarding voltages and power flows.

1.2 Problem definition

The increase in production from variable RES type distributed generators (DGs), brings several challenges to the typical fully centralised generation-transmission-distribution system. In order to overcome these difficulties, the grid must be updated in order to provide distribution grid operators the right tools to ensure a secure and stable operation. In fact, the stochastic nature of intermittent RES makes their integration and operation more complex. Therefore, a simultaneous installation of RESs, ESSs and SCBs can alleviate the issues associated with production variability and uncertainty.

Moreover, with the inclusion of RES the operation of distributed energy systems has become more complex, since traditional systems were not designed for two-way power-flows. Therefore, it is imperative to develop an operational model that optimally manages technologies such as RESs, ESSs and SCBs, that can maintain the system's reliability and meet international objectives on environmental issues.

1.3 Objectives

The main objectives of this dissertation are the following:

- To carry out a comprehensive literature review on the subject areas of operating a distribution network featuring large-scale variable RESs and ESS/SCBs integration;
- To develop a mathematical model for operating the distribution network considering the stochastic behaviour of variable RESs;
- To carry out several case studies that simulate different operation scenarios;
- To analyse the impact of variable RESs, ESSs and SCBs, both collectively or individually, in the relevant system variables;
- To determine ESS capability to manage RES uncertainty and variability, while still maintaining system stability.

1.4 Methodology

The work developed in this dissertation revolves around a quantitative and qualitative analysis regarding the optimal coordination and management of large scale RESs, ESSs and SCBs into distribution systems. In order to achieve the proposed objectives for this work, a mathematical simulation model is developed, that accounts for variable RES uncertainty and variability as well as demand variability. The proposed optimization model is of a stochastic mixed integer linear programming (SMILP) nature, aiming to optimally operate distribution network systems featuring large-scale variable renewables, and alleviate the negative impacts of RESs on the overall performance of such systems by means of ESSs and SCBs.

The problem is programmed in GAMS 24.0, and solved using the CPLEX 12.0 solver. All simulations are conducted in a HP Z820 workstation with two E5-2687W processors, each clocking at to 3.1 GHz frequency.

1.5 Dissertation Structure

The contents of the dissertation are divided in five chapters. In chapter 2, a brief historical evolution of the European electrical system is presented, as well as a definition of the main concepts used in this dissertation. Also, a literature review of relevant works on the subject area of the dissertation is presented. Chapter 3 focuses on the mathematical formulation of the operational model, where the equations, that are the pillar of this work, are presented and explained. In chapter 4 the main considerations and the methodology followed to obtain the different scenarios are presented. Furthermore, an extensive analysis of the results is done, especially in terms of costs, losses, voltages deviations and energy mix. Finally, in Chapter 5 all the relevant conclusions are presented, as well as possible future work, and works that resulted from this dissertation are highlighted.

Chapter 2

Integration of RES in Electric Power Systems

In this chapter, a general idea of the evolution of the European energy production paradigm and its future is presented. Additionally, an overview about the concepts of distributed generation (DG), renewable energy sources (RESs), switchable capacitor banks (SCBs) and energy storage systems (ESSs) is provided. Furthermore, this chapter encompasses detailed review of RES integration together with ESSs and SCBs.

2.1 European Case

2.1.1 Installed capacity

The total installed capacity in the European Union increased by 73% from 1990 to 2014. Furthermore, while in 1990 the majority of the installed capacity was based in combustible fuels (57%) that technology weight has decreased, in 2014, to 49% while wind and solar power generators increased from previously negligible values to 13% and 9% of total capacity, respectively [6].

The evolution of the installed capacity in the European Union (EU), is presented in Table 2.1.

Table 2.1: EU-28 Installed capacity (adapted from [6])

Year	1990 [MW]	2000 [MW]	2010 [MW]	2014 [MW]
Nuclear	121 070	136 637	131 731	123 515
Hydro	119 652	132 866	147 591	150 280
Tide, Wave, Ocean	240	241	241	244
Geothermal	499	604	762	820
Solar	10	179	30 149	89 088
Wind	454	12 711	84 567	129 080
Combustible Fuels	321 479	391 490	487 932	482 466
Other	10	229	883	2 164
Total	563 414	674 957	883 856	971 657

2.1.2 Energy production in the European Union

In terms of total energy production from 2010 to 2014 there was a continuous decrease in production. In fact, the peak production value happened in 2008 (3387 TWh) and in 2014 it presented a 5.8% decrease to 3191 TWh [6]. However, in 2014 the highest share of European power was produced using RES (28.2% [1]) followed by nuclear (27.5%) and coal fired power plants (25.3%).

The evolution of gross electricity production by fuel is presented in Table 2.2.

Table 2.2: EU-28 Gross electricity production by fuel (adapted from: [6])

Year	1990 [TWh]	2000 [TWh]	2010 [TWh]	2014 [TWh]
Solid fossil fuels	1 019	934	829	809
Crude oil/Petroleum products	224	181	87	57
Natural Gas and derived	224	513	799	490
Nuclear	795	945	917	876
Renewable	328	449	710	931
Waste (non-renewable)	5	12	19	23
Other	0	1	4	5
Total	2 595	3 036	3 366	3 191

Electricity generation from natural gas reached its peak in 2008 (790 TWh), however by 2014 it decreased to 457 TWh. Similarly, electricity produced using nuclear power plants showed a decrease of 13% in 2014 compared with its peak value in 2004 [6].

In Table 2.2, it is possible to observe the significant changes in the contribution of RES to electricity production since 1990. In fact, electricity generation from RES has, approximately, tripled in volume and is the only source that presents a continuous growth after 2008. Additionally, in 1990, 94% of renewable electricity was produced using hydropower plants, a share which reduced to 44% in 2014. In contrast, wind and solar power production increased to 27.2% and 9.9% of total renewable energy production, respectively, in 2014 [6].

In 2015, a similar situation regarding hydropower production was observed. Indeed, only 37% of total renewable electricity generation used this technology. This happens due to the rapid expansion of other renewable technologies (i.e. Wind and solar power production). In fact, wind power generation "more than quadrupled" from 2005 to 2015 [7]. Solar power production also increased in 2015, accounting for 12.2% of total renewable electricity.

2.1.3 RES share evolution in the EU-28

In recent years, reneweble energy has strongly grown in the EU [7]. In fact, up to 2010 a strong growth of these technologies was observed. Only in 2011, because of warm weather, difficulty in implementing the Renewable Energy Directive, and Europe's economic situation, resulted in a decrease in the use of these systems. However, the RES share in final consumption of energy increased, due to an even stronger decrease of energy produced using fossil fuels.

[1] From Table 2.2 Renewables share, in 2014, is actually 29.2%

As pictured in Figure 2.1, the share of renewable sources in gross final consumption of energy has continuously increased, representing, in 2015, 16.7%. This demonstrates the commitment towards the Europe 2020 target of 20% of renewables share in gross final energy consumption.

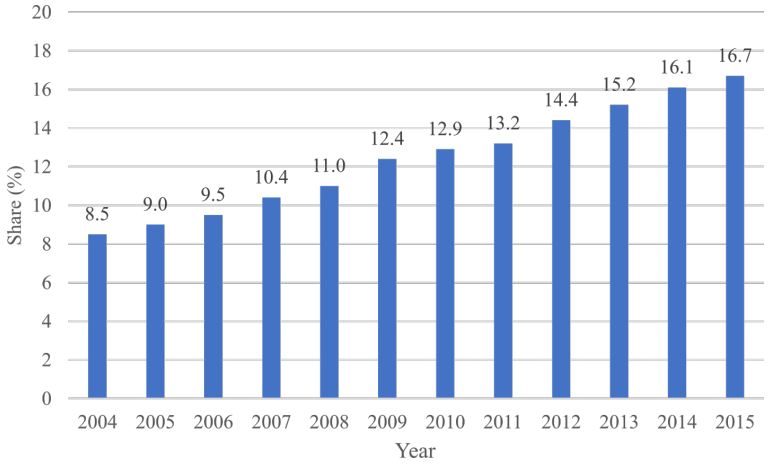

Figure 2.1: Evolution of the share of energy from RES in gross final consumption of energy

In Figure 2.2, it is possible to observe the share of energy from renewable sources, in 2015, for each of the EU member states, and their respective target to 2020.

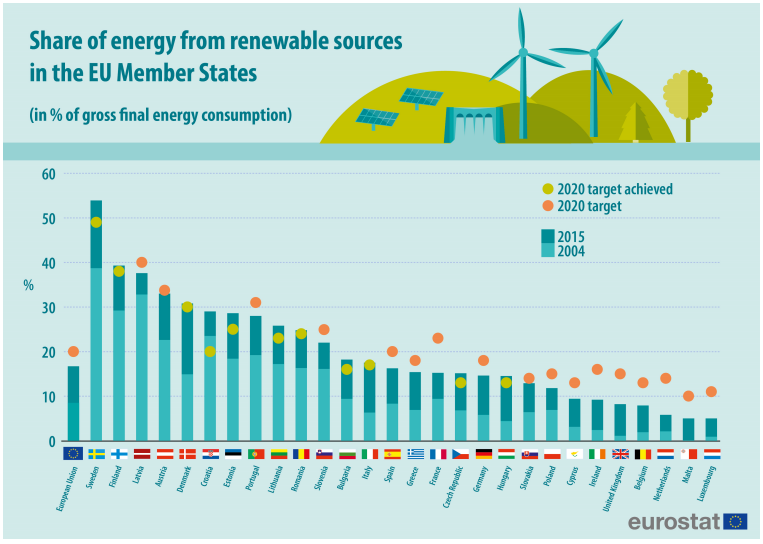

Figure 2.2: Share of energy from renewable sources per member state [7]

It is possible to observe that while some member-states have already reached the 2020 target value, other still have not implemented sufficient measures [7].

2.2 DG and RES Aspects

There are several criteria for defining DG in the literature, as pictured in Figure 2.3. However certain characteristics are common such as: electrical power generation source that is usually connected to the distribution network near the costumer [3], [8], [9]. However, the integration of such technology results in a more complex distribution network, that is mainly driven by the emerging renewable type DGs. Examples of the main factors that have increased DG significance in power systems are: constraints on the construction of new transmission lines, concerns on climate change, and electricity market liberalization.

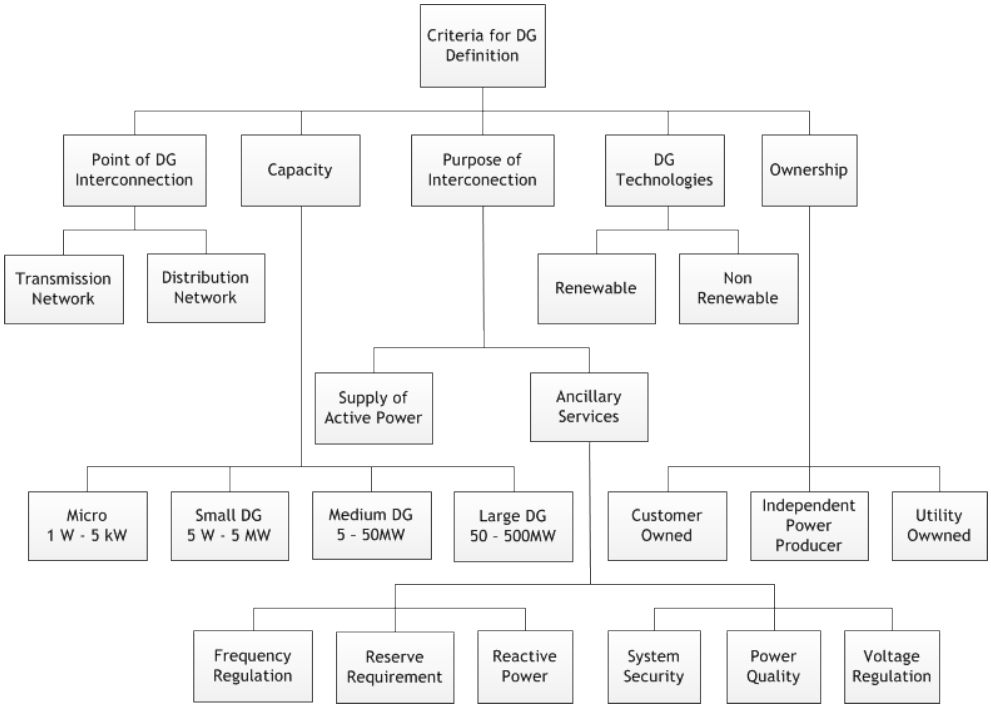

Figure 2.3: Classification of DG (adapted from: [3])

Renewable energy sources can be defined as replenishable source whose primary resource (i.e. wind speed and solar radiation) can be found worldwide. Examples of RES are: photovoltaic, wind, hydro and geothermal. Furthermore, these systems are highly associated with the concept of dispersed generation.

Wind power production is the main RES used arround the world, followed by solar power [10]. As stated in previous sections, both technologies also present a high rate of development in recent years. This is mainly due to a decreasing trend in the cost associated with RES based generation, allowing for their large scale integration [3], together with increasing environmental concerns.

However, unlike conventional systems, these technologies are strongly dependent on weather conditions [8], which are highly stochastic. Therefore, the non-dispatchable nature of these systems togheter with their rapid expansion has also impacted the levels of uncertainty and variability in the electrical system [10], [11].

In order to improve system reliability, measures are taken such as advanced metering, which allows two way communication between consumers and companies, thus increasing system management capacities. In fact, because of increased use of renewable type DGs, new concepts such as the Smart Grid and Micro Grid emerged, so that the system can efficiently respond to irregular power outputs and variable voltage profiles [11].

2.3 Technologies for Mitigating the Effects of RESs

Current energy systems have experienced significant changes in the last decade. In particular, distribution network systems are now gradually evolving from passive to active network systems. These changes are as a result of the need for the energy systems to adapt to new challenges such as the continuous increase in demand for electricity [11], environmental concerns associated with conventional power generation practices, energy transmission and distribution, etc. In order to partly overcome such challenges, DG systems (renewables, in particular) have been integrated in the energy systems, which is becoming a common practice around the world. Effectively, renewable energy sources are encouraged by several governments, in order to meet goals on climate change related issues [10].

ESSs are perceived as essential component for the operation of an increasingly complex electric grid [12]. In fact, as more RES is integrated into the system, to counter the impact of uncertainty and forecast errors, there is a need to increase reserve capacity, and this has carries additional costs. However, by implementing ESS instead of conventional generators, the aforementioned phenomenons can be mitigated. Furthermore, ESS also provides the opportunity to manage RES intermittency, which improves system reliability.

Voltage control is also a very important issue in distribution systems, and the inclusion of renewable DGs can affect voltage profiles. Therefore, important components for voltage regulation are capacitor banks, which are used to inject reactive power in order to, for example, eliminate voltage drops on long feeders [5]. This way, the use of SCBs plays a key role in maintaining voltage stability, reduce energy losses and correct the power factor of the system, which also contributes to alleviate the effects of large scale RESs integration.

Both of these technologies can be integrated in the Smart Grid concept, and provide the opportunity to manage RES intermittency, which improves system reliability.

2.3.1 Energy storage systems

Energy storage systems allow the storage of electrical energy from a power network. In this line, an ESS can be seen as a generator which consumes electricity as fuel, that is converted into potential energy that can be used later for electricity generation [12]. However, in order to store electrical energy, storage requires its conversion into another form of energy [13].

In the literature, ESSs can be classified in several types [13], such as: electrochemical, electrical and mechanical. The first type, converts chemical energy into electrical energy, through a chemical reaction between, at least, two components. Electrical type ESSs are mainly categorized

as capacitors and supercapacitors. Finally, mechanical ESSs refer to the storage of energy using the working principal of kinetic energy and potential energy, for example pumped hydro facilities. It is important to note that different ESS technologies have different efficiencies, and life cycles.

Through the use of ESSs, a strong support to renewables can be provided, such as peak demand reduction and greater penetration of RES, since normal grid operation is allowed even with considerable fluctuations in renewable power production. In addition, from a client prespective, ESSs also provide the opportunity to manage electricity costs by manipulating demand patterns [12]. Furthermore, with the continuous growth of RESs, ESSs are expected to gain importance in the near future [3].

In 2015, *Macedo et al.* [14] developed a model to solve the optimal operation problem of radial distribution systems with energy storage, where the objective function minimized the cost of energy purchase from the substation and dispatchable DG costs, using mixed-integer second order programming (MISOCP) and mixed integer linear programming (MILP). The presented model was tested on a realistic case study, and demonstrated that the MILP model presented good quality solutions allied with shorter simulation running times. However, this study does not consider: the effect of different charging and discharging efficiencies in the system, reactive power support from variable RESs and emission costs from each active power source.

Jayasekara et al. [15] focused their work on developing a strategy for the optimal integration of ESSs to improve load and DG hosting ability of the utility grid. Their work contains an economic analysis on the sizing of ESS for different operation principles.

From a different prespective, authors in [16] assess the integration of ESS in the market. In their analysis, the authors state that the current markets can sustain ESS integration, however that does not mean that current mechanisms maximize the benefits for market participants.

ESSs will be extremely important components of future power systems because they help to counteract the varability of power generated using RESs, as well as the uncertainty associated with power supply, which adversely affects the optimal operation and reliability of the traditional electrical systems [17]. Therefore, the use of ESSs allows to level the imbalance between energy generation and demand [18], [19]. In addition, ESSs can contribute to relieving the fluctuation, low voltage ride through, and voltage support, resulting in smoother power output. In [20], the wide-range benefits of using ESSs in the distribution system are extensively discussed. Despite all this, ESSs are yet very expensive. However, with the continuous technological development, the cost of most ESS technologies has been decreasing with high learning rates. A recent study on cost-benefit analysis of ESSs has shown that ESSs are becoming increasingly competitive, and the use of such technologies is justified in many cases [20].

2.3.2 Switchable capacitor banks

Another technology that allows greater integration and management of RESs is switchable capacitor bank. This is due to the fact that power systems require a significant amount of reactive power to maintain the voltage in the nodes within specified ranges. There are several switching methods such as the VAR compensation source but the most commonly used is switchable capacitor

banks since capacitors are passive filters and do not interfere with the optimization process [21]. Therefore, capacitor banks are widely used and effective technologies, both at the transmission and distribution levels.

In the literature, several positioning techniques of capacitor banks have been proposed as in [22–24]. In [5] *Homaee et al.* proposed two different models for real-time voltage control algorithms based on controllable capacitor banks fitted with remote terminal units. *Ameli et al.* [25] developed a model for simultaneous dynamic feeder reconfiguration and capacitor bank switching.

In addition to maintaining the nodal voltages at standard levels, capacitor banks can be used to reduce energy losses by injecting reactive power into the system [22], thereby increasing system capacity and correcting system power factor [26]. Capacitor banks placement along the line will compensate for the inductive nature of the line and reactive loads [27]. Therefore, SCBs will help maintain the stability and integrity of distribution networks systems, as well as the power quality in the system.

2.3.3 The future development of RES

The integration of RES type DGs is perceived as a solution to decrease fossil fuel dependency and provide a solution to a growing energy demand [3]. Furthermore, energy resources such as wind and solar, are abundantly avaliable in nature, and can be exploited in large scale in a sustainable manner. The difusion of RES should also help to counter the risks of volatibility of fossil fuel prices or of geoplitical pressures [8].

In this line, RESs are and will continue to be an important part of the process of finding "cleaner" power sources. In fact, for example, EU countries agreed on a new renewable energy target of at least 27% of final energy consumption by 2030 [7].

However, the integration of variable RES comes with several challenges, both economic and technical. On the technical side, the first major challenge that immediately comes with RES integration is related to the uncertainty and variability of renewables, which “make the management of network systems very difficult” [28]. Furthermore, violations of system-wide technical restrictions are not tolerated especially at distribution levels, that is, the system should always operate respecting the technical limitations [29]. On the economical point of view, the non-dispatchable nature of RES, especially wind and solar, brings additional costs. To overcome these challenges several countries are investing in planning and expanding their current infrastructure to cope with RES integration [10].

It is necessary to introduce technologies that facilitate the integration variable RESs and their effective management. Among others, the optimal use of ESSs and SCBs is a viable option capable of addressing the aforementioned challenges, at least partly.

2.4 Chapter Summary

The increased use of RES brings several challenges to the distribution grid, and it is very important to allocate and manage all of the available resources to ensure a stable integration of RES. The uncertainty that characterizes RES, especialy wind power, the most widely used source of renewable energy [10], plays a significant role on the management and stability of such systems.

To overcome these challenges it is expected that distribution grids will undergo a transformation process from passive to active, that is, the evolution to smart grids. This transformation will enable smart grid technologies (storage and switchable capacitor banks), that will need to be managed in order to ensure a certain flexibility, which will ease the management of RES uncertainty and variability. Moreover, as new components are being integrated to the grid, the necessity for new operational guidelines emerges.

Chapter 3

Mathematical Formulation

The objective of this work is to investigate an optimal operation of distribution grids featuring large-scale RES based DGs, SCBs, and ESSs. To this end, this work develops a new stochastic MILP model that aims to ensure a more efficient utilization of variable renewables at distribution levels. In addition, the model is used for managing the uncertainty inherent to such energy sources with properly located ESSs and SCBs, thereby maintaining the stability and the integrity of distribution networks systems as well as the power quality in the system.

3.1 Objective Function

The objective function minimizes the sum of expected costs of operation, unserved power and emissions along the optimization scope:

$$Min\ TC = COT + CUT + CET \tag{3.1}$$

where the weights δ_n are considered in objective function in order to account for the relative importance of each cost. In this study, their are all set to 1. However, it is at the operator's discretion to associate different weights for the cost terms in (3.1).

The total operation cost is given by the sum of expected costs of power generated by DGs, imported and discharged power as:

$$\begin{aligned} COT = & \sum_{s\in\Omega^s} \rho_s * \sum_{h\in\Omega^h} \sum_{g\in\Omega^g} \sum_{i\in\Omega^i} OC_{g,i,s,h} * P_{g,i,s,h} \\ & + \sum_{s\in\Omega^s} \rho_s * \sum_{h\in\Omega^h} \sum_{\zeta\in\Omega^\zeta} \lambda^{\zeta}_{s,h} * P^{SS}_{\zeta,s,h} \\ & + \sum_{s\in\Omega^s} \rho_s * \sum_{h\in\Omega^h} \sum_{es\in\Omega^{es}} \sum_{i\in\Omega^i} \lambda^{dch}_{s,h} * P^{dch}_{es,i,s,h} \end{aligned} \tag{3.2}$$

where ρ_s is the probability of scenario s, given by the product of individual probabilities of wind, solar and demand scenarios, i.e $\rho_s = \rho_{dem} * \rho_{sol} * \rho_{win}$. $OC_{g,i,s,h}$ is the operation cost of unit energy production by DGs (€/MWh); $P_{g,i,s,h}$ is the active power produced by DGs; $\lambda^{\zeta}_{s,h}$ is the price of

electricity purchased from upstream (€/MWh); $P^{SS}_{\zeta,s,h}$ is the active power imported from the grid (MW); $\lambda^{es}_{s,t}$ the variable cost of storage units that accounts for the degradation of the energy storage system; $P^{dch}_{es,i,s,h}$ the discharged power from storage; and $u_{es,i,h}$ is a control variable, set to 1 in this study, that defines whether a storage unit is connected or not.

Note that the third term in (3.2) only multiplies the "useful" discharge power with the corresponding cost. To directly model the cost of total discharge (including ESS discharging losses), this product should be multiplied by $1/\eta^{dch}_{es}$. However, to ensure the same treatment as other power sources, the efficiency of ESS is not directly considered in the cost of operation of such units, but it affects the cycle of charge and discharge (3.26) which in turn affects the power flow equations.

To model the total cost of unserved power, penalties $v^{P}_{s,h}$ and $v^{Q}_{s,h}$ are considered for active and reactive power, receptively:

$$\begin{aligned} CUT = &\sum_{s\in\Omega^s} \rho_s * \sum_{h\in\Omega^h} \sum_{i\in\Omega^i} v^{P}_{s,h} * P^{un}_{i,s,h} \\ &+ \sum_{s\in\Omega^s} \rho_s * \sum_{h\in\Omega^h} \sum_{i\in\Omega^i} v^{Q}_{s,h} * Q^{un}_{i,s,h} \end{aligned} \tag{3.3}$$

The variables $P^{un}_{i,s,h}$ and $Q^{un}_{i,s,h}$ refer to the active and reactive unserved power, respectively.

The final term that is part of the objective function, refers to total cost of emissions. It is modeled as:

$$\begin{aligned} CET = &\sum_{s\in\Omega^s} \rho_s * \sum_{h\in\Omega^h} \sum_{g\in\Omega^g} \sum_{i\in\Omega^i} \lambda^{CO2}_{s,h} * ER_g * P_{g,i,s,h} \\ &+ \sum_{s\in\Omega^s} \rho_s * \sum_{h\in\Omega^h} \sum_{\zeta\in\Omega^\zeta} \lambda^{CO2}_{s,h} * ER_{SS} * P^{SS}_{\zeta,s,h} \end{aligned} \tag{3.4}$$

In the above equation, $\lambda^{CO2}_{s,h}$ refers to the price of emissions (€/tCO_2), ER_g and ER_{SS} denote the emission rates of DGs and substation, respectively (tCO_2/MWh).

3.2 Constraints

3.2.1 Kirchhoff's voltage law

Power flows in all feeders need to be governed by Kirchoff's voltage law, the so-called AC power flow equations.

$$P_l = V_i^2 g_l - V_i V_j (g_l \cos\theta_l + b_l \sin\theta_l) \tag{3.5}$$

$$Q_l = -V_i^2 b_l + V_i V_j (b_l \cos\theta_l - g_l \sin\theta_l) \tag{3.6}$$

$$V_i = V_{nom} + \Delta V_i, \text{ where } \Delta V^{min} \leq \Delta V_i \leq \Delta V^{max} \tag{3.7}$$

These equations are however highly nonlinear and non-convex, making it difficult to integrate such constraints in complex problems similar to the one addressed in this study. For this reason,

they are often linearised under various simplifing assumptions. Here, the linearised AC network model proposed in [30] is being considered, but adapting it to fit the point of view of the operation of the system.

These equations are often linearised by considering two practical assumptions. Firstly, bus voltage magnitudes are expected to be close to the nominal value V_{nom}. The second assumption concerns the voltage angle difference θ_l, across a line, which is often very small, leading to the trigonometric approximations $\sin\theta_l \approx \theta_l$ and $\cos\theta_l \approx 1$. These approximations are valid as this study refers to distribution systems where the active power flow dominates the apparent power flow in lines. Note that θ_l represents the angle difference between two nodes of the same branch $(\theta_i - \theta_j)$ where i stands for the sending node and j for the receiving node.

Additionally, voltage magnitudes are expected to be very close to the nominal voltage, then voltage deviations (ΔV_i) at each node are expected to be very small. Substituting (3.7) in (3.5) and (3.6), and neglecting higher order terms:

$$\begin{aligned} P_l \approx\ & (V_{nom}^2 + 2V_{nom}\Delta V_i)g_l \\ & - (V_{nom}^2 + V_{nom}\Delta V_i + V_{nom}\Delta V_j)(g_l + b_l\theta_l) \end{aligned} \tag{3.8}$$

$$\begin{aligned} Q_l \approx\ & -(V_{nom}^2 + 2V_{nom}\Delta V_i)b_l \\ & + (V_{nom}^2 + V_{nom}\Delta V_i + V_{nom}\Delta V_j)(b_l - g_l\theta_l) \end{aligned} \tag{3.9}$$

Equations (3.8) and (3.9) still contain nonlinearities due to the product of two continuous variables (voltage deviations and angle differences). As these variables are very small, their product can be neglected, which leads to the following simplification:

$$P_{l,s,h} \approx V_{nom}(\Delta V_{i,s,h} - \Delta V_{j,s,h})g_l - V_{nom}^2 b_l(\theta_{l,s,h}) \tag{3.10}$$

$$Q_{l,s,h} \approx -V_{nom}(\Delta V_{i,s,h} - \Delta V_{j,s,h})b_l - V_{nom}^2 g_l(\theta_{l,s,h}) \tag{3.11}$$

3.2.2 Power flow limits

Considering the apparent power flow through a line, that is given by $S_l = \sqrt{P_l^2 + Q_l^2}$, and knowing that it has to be less or equal to the rated value, then the thermal limit in a feeder is given by:

$$P_{l,s,h}^2 + Q_{l,s,h}^2 \leq (S_l^{max})^2 \tag{3.12}$$

The quadratic expression (3.12) is linearised using a piecewise linearization approach, considering a sufficient number of linear segments, Y. In this study, Y is considered equal to 5, a number which balances accuracy with computation burden [31]. There are several ways of linearizing such functions as described in [32]. This approach is based on the first-order approximation of a non-linear curve, and is chosen due to its relatively simple formulation. In order to reduce the mathematical complexity of the formulation, two non-negative auxiliary variables are introduced for each of the flows P_l and Q_l, such that $P_l = P_l^+ - P_l^-$ and $Q_l = Q_l^+ - Q_l^-$. These auxiliary variables (P_l^+, P_l^-, Q_l^+ and Q_l^-) represent the positive and negative flows of P_l and Q_l, respectively.

The associated linear constraints, in this case, are presented below:

$$P^2_{l,s,h} \approx \sum_{y=1}^{Y} \alpha_{l,y} p_{l,s,h,y} \tag{3.13}$$

$$Q^2_{l,s,h} \approx \sum_{y=1}^{Y} \beta_{l,y} q_{l,s,h,y} \tag{3.14}$$

$$P^+_{l,s,h} + P^-_{l,s,h} = \sum_{y=1}^{Y} p_{l,s,h,y} \tag{3.15}$$

$$Q^+_{l,s,h} + Q^-_{l,s,h} = \sum_{y=1}^{Y} q_{l,s,h,y} \tag{3.16}$$

where $p_{l,s,h,y} \leq P^{max}_l / Y$ and $q_{l,s,h,y} \leq Q^{max}_l / Y$.

3.2.3 Line losses

The active and reactive power losses in line l can be approximated as:

$$\begin{aligned} PL_l &= P_{l,ij} + P_{l,ji} \approx 2 * V^2_{nom} g_l (1 - \cos\theta_l) \\ &\approx V^2_{nom} g_l \theta^2_l \end{aligned} \tag{3.17}$$

$$\begin{aligned} QL_l &= Q_{l,ij} + Q_{l,ji} \approx -2 * V^2_{nom} b_l (1 - \cos\theta_l) \\ &\approx -V^2_{nom} b_l \theta^2_l \end{aligned} \tag{3.18}$$

To ease the analysis of the difference between incoming and outgoing power flows, from the point of view of the line, $P_{l,ij}$ represent the line power flow seen from the sending end of the line, while $P_{l,ji}$ stands for the power flow seen from the receiving end of the same line.

Equations (3.17) and (3.18) can be expressed in terms of active and reactive power flows as in:

$$PL_{l,s,h} = r_l (P^2_{l,s,h} + Q^2_{l,s,h}) / V^2_{nom} \tag{3.19}$$

$$QL_{l,s,h} = x_l (P^2_{l,s,h} + Q^2_{l,s,h}) / V^2_{nom} \tag{3.20}$$

Expressing losses as a function of power flows reduces the number of nonlinear terms, which, in turn reduces the number of variables and equations required. The details related to equations (3.19) and (3.20) are included in Appendix A.

3.2.4 Active and reactive load balances

To ensure that, at all time, load balances are respected, the sum of of all injections should be equal to the sum of all withdrawals at each node for both active (3.21) and reactive (3.22) power, which

is the so called *Kirchhoff's Current Law*:

$$\begin{aligned} &P^{SS}_{\zeta,s,h} + \sum_{g\in\Omega^{DG}} P_{g,i,s,h} + \sum_{es\in\Omega^{es}} (P^{dch}_{es,i,s,h} - P^{ch}_{es,i,s,h}) + \sum_{in,l\in i} P_{l,s,h} - \sum_{out,l\in i} P_{l,s,h} + P^{un}_{i,s,h} \\ &= DemP^{i}_{s,h} + \sum_{in,l\in i} \frac{1}{2} PL_{l,s,h} + \sum_{out,l\in i} \frac{1}{2} PL_{l,s,h} \; ; \forall\, \zeta \in i \end{aligned} \tag{3.21}$$

$$\begin{aligned} &Q^{SS}_{\zeta,s,h} + \sum_{g\in\Omega^{DG}} Q_{g,i,s,h} + \sum_{cb\in\Omega^{cb}} Q^{cb}_{i,s,h} + \sum_{in,l\in i} Q_{l,s,h} - \sum_{out,l\in i} Q_{l,s,h} \\ &= DemQ^{i}_{s,h} + \sum_{in,l\in i} \frac{1}{2} QL_{l,s,h} + \sum_{out,l\in i} \frac{1}{2} QL_{l,s,h} \; ; \forall\, \zeta \in i \end{aligned} \tag{3.22}$$

In the above equations, $DemP^{i}_{s,h}$ and $DemQ^{i}_{s,h}$ represent the active and reactive power demand, respectively, at node i. Active and reactive power losses are represented at each end of the line, with half of the total amount for the corresponding line.

3.2.5 Energy storage model

ESS constraints are presented below:

$$0 \le P^{ch}_{es,i,s,h} \le u_{es,i,h} I^{ch}_{es,i,h} P^{ch,max}_{es,i,s,h} \tag{3.23}$$

$$0 \le P^{dch}_{es,i,s,h} \le u_{es,i,h} I^{dch}_{es,i,h} P^{dch,max}_{es,i,s,h} \tag{3.24}$$

$$I^{ch}_{es,i,h} + I^{dch}_{es,i,h} \le 1 \tag{3.25}$$

$$\begin{aligned} E_{es,i,s,h} &= E_{es,i,s,h-1} + \eta^{ch}_{es} P^{ch}_{es,i,s,h} \\ &\quad - \beta^{dch}_{es} P^{dch}_{es,i,s,h}, \;\; \text{where } \beta^{dch}_{es} = \frac{1}{\eta^{dch}_{es}} \end{aligned} \tag{3.26}$$

$$E^{min}_{es,i,s,h} u_{es,i,h} \le E_{es,i,s,h} \le E^{max}_{es,i,s,h} u_{es,i,h} \tag{3.27}$$

$$E_{es,i,s,h_0} = \mu_{es} u_{es,i,h} E^{max}_{es,i} \tag{3.28}$$

$$E_{es,i,s,h_f} = E_{es,i,s,h_0} \tag{3.29}$$

The charging and discharging limits related to ESS are depicted in (3.23) and (3.24), respectively. Note that $u_{es,i,h}$ is a control variable, set to 1 in this study, that defines if a storage unit is connected or not.

Constraint (3.25) ensures that charging and discharging cannot occur simultaneously, since binary charging and discharging indicators ($I^{ch}_{es,i,h}$ and $I^{dch}_{es,i,h}$, respectively) are used. The amount of energy available in ESS at hour h depends on the state of charge at the previous hour and on the charge or discharge cycle, on hour h, as demonstrated in (3.26). The maximum and minimum storage capacity at hour h are also considered in (3.27). Constraints (3.28) and (3.29) ensure that there is an initial charge storage level (3.28), and that at the end of the cycle (h_f) the amount of energy stored is the same as the initial ESS level (3.29). These constraints ensure that the obtained solution does not depend on the initial reservoir level. The parameter μ_{es} refers to the initial percentage of stored energy.

Charging and discharging inefficiencies are considered in order to model losses (electrical, chemical, etc.) and discharging losses. In other words, more energy is required to charge ESS and less energy is withdrawn from ESS due to charging and discharging losses, respectively. This is the reason why $1/\eta_{es}^{dch}$ is associated with discharging power in equation (3.26). In this study, charging (η_{es}^{ch}) and discharging (η_{es}^{dch}) efficiencies are considered equal.

The larger number of discrete variables in the storage model can render significant computational burden. In order to overcome this level of complexity, equations (3.23), (3.24) and (3.25) are substituted by a relaxed version without charging and discharging indicators, as follows:

$$0 \leq P_{es,i,s,h}^{ch} \leq u_{es,i,h} P_{es,i,s,h}^{ch,max} \tag{3.30}$$

$$0 \leq P_{es,i,s,h}^{dch} \leq u_{es,i,h} P_{es,i,s,h}^{dch,max} \tag{3.31}$$

Under normal conditions, the ESS model with (3.30) and (3.31) is exact, since by the principle of optimality it does not make economical sense to have both $P_{es,i,s,h}^{ch}$ and $P_{es,i,s,h}^{dch}$ greater than zero at the same time.

3.2.6 DG active and reactive power limits

Active and reactive power limits related to DGs are presented below:

$$0 \leq P_{g,i,s,h} \leq P_{g,i,s,h}^{max} \tag{3.32}$$

$$0 \leq Q_{g,i,s,h} \leq Q_{g,i,s,h}^{max} \tag{3.33}$$

In the case of variable power generation sources, $P_{g,i,s,h}^{max}$ should be equal to the actual production at a specific hour because these type of sources depend on the level of primary energy sources such as solar radiation or wind speed. In this study, wind and solar PV type DGs are considered to have reactive power support capabilities. For example, DFIG based wind turbine and voltage source inverter based PV have such capabilities and are expected to be widely integrated in distribution grids . To model this, the following constraint must be considered:

$$-\tan(\cos^{-1}(pf_g)) * P_{g,i,s,h} \leq Q_{g,i,s,h} \leq \tan(\cos^{-1}(pf_g)) * P_{g,i,s,h} \tag{3.34}$$

In (3.34), it can be observed that, the DGs are capable of operating between a leading and lagging power factor. This means that such DGs can either produce or "consume" reactive power depending on the operational situation in the system.

3.2.7 Reactive power limits at substation

The reactive power at the substation is constrained as:

$$Q^{SS,\,min}_{\zeta,s,h} \leq Q^{SS}_{\zeta,s,h} \leq Q^{SS,\,max}_{\zeta,s,h} \tag{3.35}$$

where the minimum and maximum reactive power limits are calculated as:

$$Q^{SS,\,max}_{\zeta,s,h} = \tan(\cos^{-1}(pf_{ss})) * P^{SS}_{\zeta,s,h} \tag{3.36}$$

$$Q^{SS,\,min}_{\zeta,s,h} = -\tan(\cos^{-1}(pf_{ss})) * P^{SS}_{\zeta,s,h} \tag{3.37}$$

Note that the equations above are only valid for positive $P^{SS}_{\zeta,s,h}$, since a negative value would lead to infeasibility due to constraint (3.35). This means that in this model active power export to the upstream grid is not allowed, unless otherwise mentioned.

3.2.8 Reactive power limits of capacitor banks

The following constraint related to capacitor banks models the discrete behaviour of these systems:

$$Q^{cb}_{i,s,h} = 0.1 * \sum_{c(i)}^{N_{c(i)}} X_c(i,s,h,c(i)) \tag{3.38}$$

$$X_c(i,s,h,c(i)) \leq X_c(i,s,h,c(i)-1) \tag{3.39}$$

where $c(i)$ represents a variable set depending on the location of the SCB.

Since SCB can be connected in blocks of 0.1 MVAr, depending on the location (bus i) there will be a differer number of maximum available blocks ($N_{c(i)}$).Therefore, it is possible to conclude that, by modelling SCB as in (3.38), the maximum and minimum limits are already included. Furthermore, $X_c(i,s,h,c(i))$ is a vector of binary variables which represents if a block is engaged (1) or not (0).

By using binary variable it is possible to obtained the total reactive power dispatch from SCBs, since the sum of engaged blocks multiplied by the installed capacity of each block results in the total amount dispatched. Additionally, to ensure SCB blocks are engaged in order, constraint (3.39) is also included.

However, the mathematical model for discrete SCBs significantly increases computational burden, since several new variables and variable sets are added.

In order to decrease computational burden, the discrete modelling of SCBs is replaced by a continuous model as in (3.40).

$$0 \leq Q^{cb}_{i,s,h} \leq Q^{cb,\,max}_{i} \tag{3.40}$$

3.3 Chapter Summary

This chapter has presented a detailed description of the stochastic optimization model developed here to investigate the performance of distribution grids featuring large-scale variable RESs. The effective management of variability and uncertainty introduced by such resources is the aim of the analysis. For this, the developed model encompasses ESS, and SCB technologies as well as RES-based DGs with reactive power support capabilities. The resulting optimization is of mixed integer programming nature based on a linearised AC network model, which can be solved by commercial solvers. To evaluate the proposed model and carry out the required analysis a standard IEEE 41-bus distribution system is used.

The results and analysis of different power production and demand scenarios, as well as the location of the different power production technologies, are presented in the following chapter.

Chapter 4

Case Study, Results and Discussions

The mathematical formulation presented in the last chapter will be applied to the case study in this chapter. Moreover, the obtained results will be present and discussed in terms of voltage deviation profiles, costs, losses and energy mix.

4.1 System Data Assumptions

To test the proposed operation model, an IEEE 41-bus system is used. The nominal voltage of the system is 12.66 kV, and the total active and reactive load are 4.635 MW and 3.25 MVAr, respectively. Detailed information concerning the test system can be found in the Table B.1 of Appendix B.

As described in [33], the optimal location and size of the different resources are already predetermined. However, the installed wind capacity on bus 14 has been altered to 2 MW, instead of 3 MW, to better evaluate the impact of ESS in the management of RES variability. In this study, all DGs are assumed to have reactive power support capabilities, with a power factor of 0.95.

The power factor at the substation is considered to be 0.8. This power factor, despite unrealistic, is chosen to ensure that, in the base case, all of the reactive power demand is met. Note that, in the base case, all DGs, SCBs and ESSs are not connected. This way, the only available power comes from the upstream grid, which means that there would be unserved reactive power demand in the event of high power factors. To ease the analysis of different cases and scenarios, the minimum power factor at the substation level has been maintained at 0.8.

The locations and installed capacities of different technologies are presented in Figure 4.1 and Table 4.1.

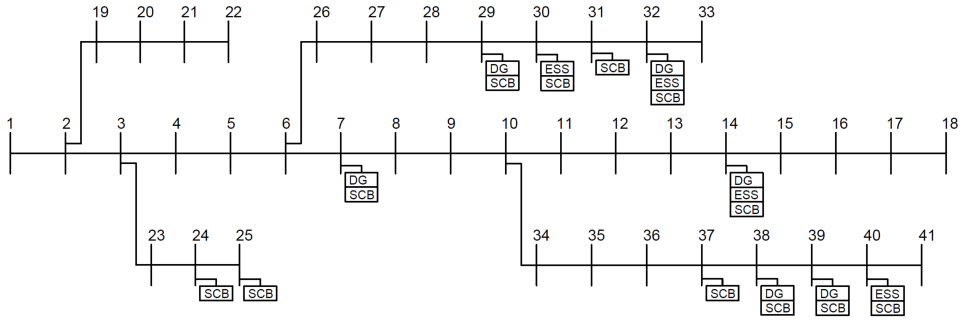

Figure 4.1: Single-line diagram of the IEEE 41-bus distribution network system and the location of different technologies

Table 4.1: Optimal locations and installed capacities of distributed energy resources

Bus	Wind	PV	ESS
7	1	0	0
14	2	0	2
29	1	0	0
30	0	0	1
32	1	1	1
38	1	1	0
39	1	0	0
40	0	0	1
Total [MW]	7	2	5

To partly meet the large reactive power requirement in the system, there are also SCBs installed throughout the system as demonstrated in Table 4.2.

Table 4.2: Optimal reactive power sources' locations and installed capacities

Bus	SCB
7	0.9
14	1.3
24	0.1
25	0.3
29	0.3
30	1
31	0.2
32	0.5
37	0.1
38	2
39	0.1
40	0.6
Total [MVAr]	7.4

In addition, the following assumptions have been made when carrying out the simulations:

- A 24 hour period has been considered;
- It is assumed that electricity price follows the same trend as demand;
- Voltage deviations must be bound between 5% and -5% of the nominal voltage;
- The number of partitions (Y) is set equal to 5 [31];
- The electrochemical type ESS is being considered;
- ESS efficiency is considered to be 90%, unless otherwise mentioned;
- A unit 1.0 MW bulk ESS with a reservoir capacity of 5 MWh is considered. At node 14 there are two ESS units of this type;
- The emission rate of power purchased is set to 0.4 tCO_2e/MWh;
- The emission rates of DGs are set to 0.0276 and 0.0584 tCO_2e/MWh for wind and solar types, respectively;
- The emission price is set to 6 €/tCO_2e;
- The electricity tariffs of wind and solar power generators are 20 and 40 €/MWh, respectively;
- The cost of discharge of ESS is set to 5 €/MWh;
- At node 1, the voltage magnitude is set to V_{nom} and the respective angle to 0;
- The cost of unserved power is set to 3000 €/MW;
- The discrete nature of SCBs is relaxed for computational reasons.

4.2 Scenario Description

As mentioned in previous chapters, the problem addressed in this thesis is subjected to various sources of uncertainty and variability. The most relevant ones are demand, wind and solar power outputs. In addition to the natural variability of such parameters, the operational model needs to account for their partial unpredictability. This is handled by taking 30 scenarios for each. However, due to computational limitations, the number of individual scenarios are reduced to 10 by means of K-means clustering technique.

The combination of the 10 individual scenarios, representing the uncertainty related to demand, wind and solar power outputs, leads to a total of 1000 scenarios.

Graphics related to scenarios present the correspondent factor for each hour. This means that the demand/production value at a specific hour will depend on the peak demand/installed capacity multiplied by a factor.

4.2.1 Demand scenarios

Demand scenarios are obtained by folding the hourly electricity consumptions profiles of the aggregate demand in Azores Islands (Portugal). As it can be seen Figure 4.2 the 10 demand scenarios are presented. As it can be seen in this figure, the average low and peak demand occur at hour 5 (48.8%) and 20 (90.3%), respectively. However, it should be noted that the 6^{th} demand scenario has the highest peak demand at hour 19 (99.8%), while scenarios 8 and 3 have the lowest (59.6%) and highest (77.2%) average daily demand, respectively.

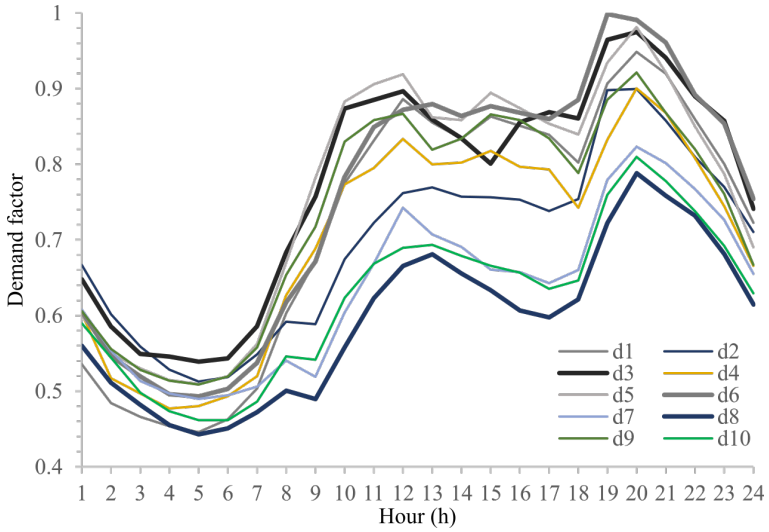

Figure 4.2: Demand scenarios considered in the study

4.2.2 Wind power production scenarios

In order to generate wind power output scenarios, different synthetic hourly wind speed data are first generated according to the method in [34]. Then, these data are translated into power using appropriate wind power model [35], [36]. The initial number of scenarios is 30, though this is reduced to 10 to ensure problem tractability. These scenarios are shown in Figure 4.3. As it can be seen, lowest and highest average power production by wind power sources occur in scenario 3 (41.5%) and 4 (51.6%), respectively.

Scenario 9 is characterized by low power production at early and late hours, and has the highest consecutive slope between hour 10 and 13 where it reduces from 54.2% to 25.8%. This means that at hour 13, wind power production is less than half that of hour 10.

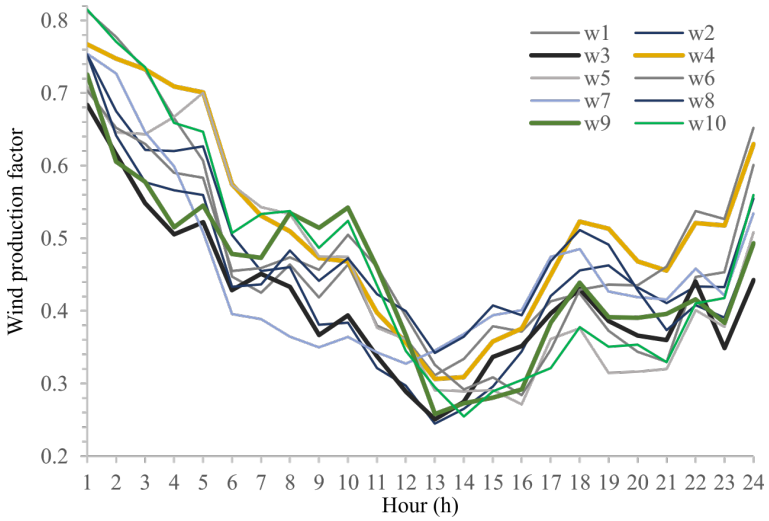

Figure 4.3: Wind power production scenarios considered in the study

4.2.3 Solar power production scenarios

Solar power production scenarios are based on realistic data from several locations in the Azores Islands. In fact, hourly solar irradiation data are taken from different locations in this islands for a length of one month (30 days). Then, the average of the hourly data is formed. Finally, as in the case of demand, the hourly profiles of each day are folded into a single day forming 30 scenarios. This is done in order to account for the uncertainty of such energy resources. The power output corresponding to each irradiation is then computed by employing the appropriate power curve [37]. Furthermore, in order to lessen the computational burden, the K-means clustering technique is applied to reduce the number of scenarios to 10.

As it can be observed in Figure 4.4, the chosen scenarios have high variability and cover a wide range of solar power production situations. The highest average solar power production occurs in scenario 2 while the lowest production levels occurs in scenario 4.

Both solar power production scenarios 2 and 9 shall be studied in detail along with with high demand and high wind power production variability. In fact, solar production scenario 9 decreases almost at the same time as wind production scenario 9, which brings additional challenges since this happens during high demand.

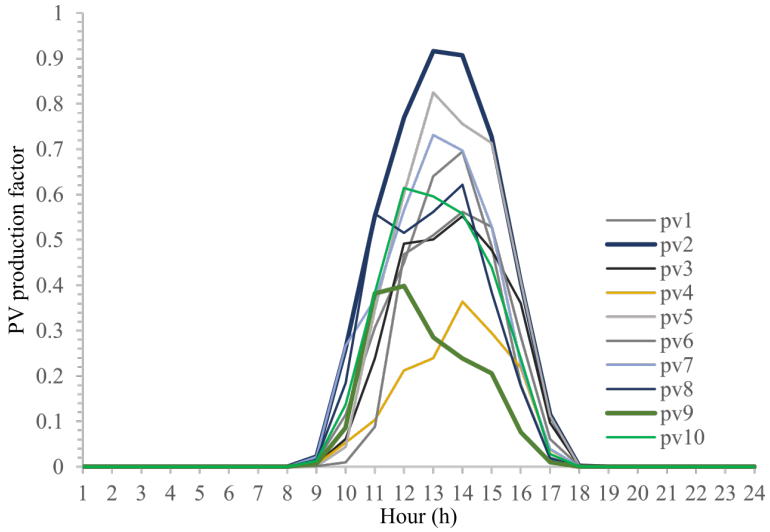

Figure 4.4: Solar power production scenarios considered in the study

4.2.4 Price Data

In Figure 4.5, it is possible to observe that the prices of purchased power varies during the 24 hour period and are considered to be correlated with demand. These data are obtained from the Italian electricity market, corresponding to a day in December 2016.

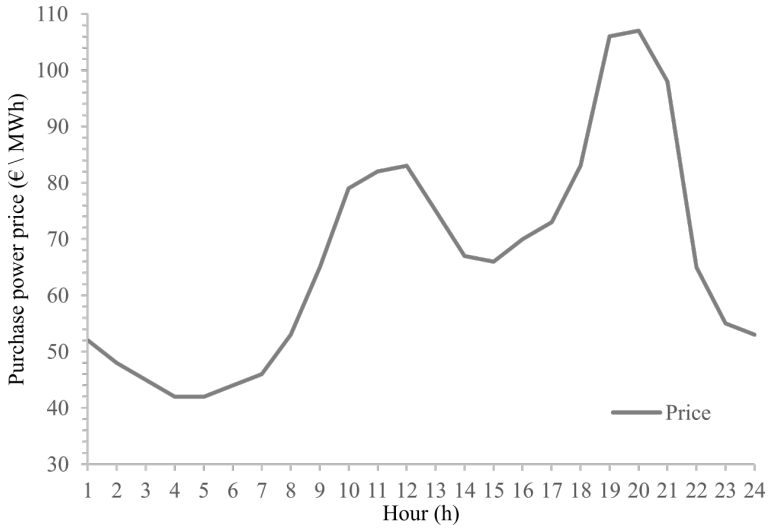

Figure 4.5: Price data

4.3 Results and Discussions

Analysis of the results will be based on hourly average values, since for each hour there are 1000 different scenarios. For voltage deviations, the illustrations will present the upper and lower bound profiles as well as the average profile. Note that upper and lower bounds refer to average voltage profiles of specific hours while "AVG" stands for the average of voltage deviations profiles of all 24 hours.

In order to analyse the behaviour and impact of DGs, ESSs and SCBs on the system, several cases are considered:

- Base case: Only importing power from the upstream grid is considered, while DGs, ESSs and SCBs are not connected.
- CB only: Only SCBs are connected, while DGs and ESSs are not.
- No ESS: Only SCBs and DGs are connected, while ESSs are not.
- Efficiency (EFF) 0.9: DGs, ESSs and SCBs are connected. Storage efficiency is set to 90%.
- EFF 0.8: The same as case "EFF 0.9", but ESS efficiency is reduced to 80%.
- EFF 0.7: The same as case "EFF 0.9", but ESS efficiency is reduced to 70%.
- No limit Q: The same as case "EFF 0.9", but constraints related to reactive power at the substation are not considered.

For each case, other than the "No limit Q" one, reactive power constraints were considered. The purpose of removing these constraints for the last case is to observe the behaviour of the system when active power export is allowed.

Emissions and import costs for each case, as well as the corresponding average losses are presented in Table 4.3.

Table 4.3: Relevant system variables for each case

Case	Base	CB only	No ESS	EFF 0.9	EFF 0.8	EFF 0.7	No limit Q
Operation Cost [€]							
DG	0.00	0.00	1487.60	1667.83	1699.13	1724.28	1788.28
ESS	0.00	0.00	0.00	52.84	43.25	29.08	67.87
Cost import [€]	5999.80	5842.75	887.39	180.65	267.27	364.29	-214.14
Cost unserved [€]	0.00	0.00	0.00	0.00	0.00	0.00	0.00
Cost of Emissions [€]							
DG	0.00	0.00	12.42	13.88	14.15	14.38	14.92
Substation	205.87	200.34	25.51	7.67	10.33	12.62	2.66
Total Cost [€]	6205.67	6043.09	2412.92	1922.87	2034.13	2144.65	1659.58
Average Losses							
PL [MW]	0.33	0.23	0.07	0.10	0.09	0.09	0.15
QL [MVAr]	0.23	0.17	0.06	0.08	0.08	0.07	0.11

4.3.1 Base case

It can be observed in Figure 4.6 that, for the base case, average voltage deviations surpass the minimum limit due to the high reactive power requirement in the system. To avoid infeasibility, in addition to lowering the power factor of the substation to 0.8, there is a need to remove the minimum voltage deviation constraint, only for the base case. However, it is important to note that the actual average substation power factor for the 24 hour period is 0.82.

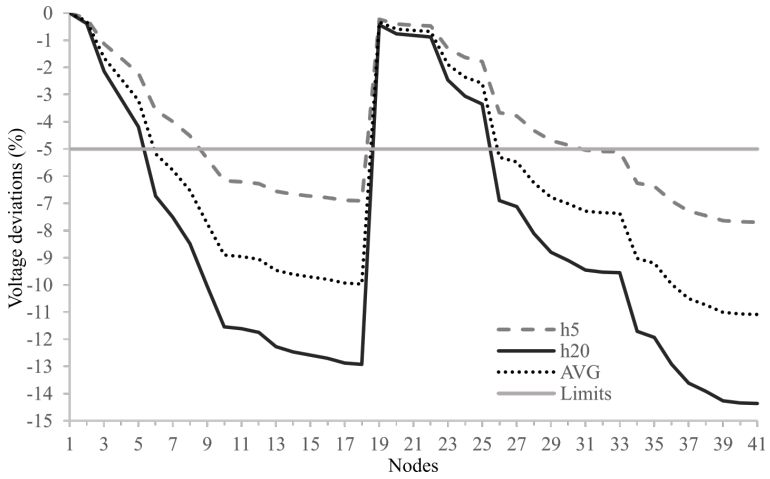

Figure 4.6: Average voltage deviations at each node for the Base case

As expected, for the base case, where only import is considered, average voltage deviations increased throughout the system, especially for buses far away from the substation, as it can be seen Figure 4.6. Furthermore, bus 1 is considered to have a deviation of 0%, then all downstream buses will have a negative voltage deviation, as power flows from upstream to downstream, a classic system power flow. As a result, the average voltage deviation at bus 41 could vary between -7.7% and -14.3% for low and high demand hours, respectively.

Observing Figure 4.7, it possible to conclude that import share represents 100% of the energy mix. As a result, there is only a high cost of imported energy and the respective emission cost. In fact, this case presents the highest total cost and highest average value of both active and reactive power losses, as seen in Table 4.3. Losses in the system can also be observed in Figure 4.7 through the difference in the actual power production and demand profiles.

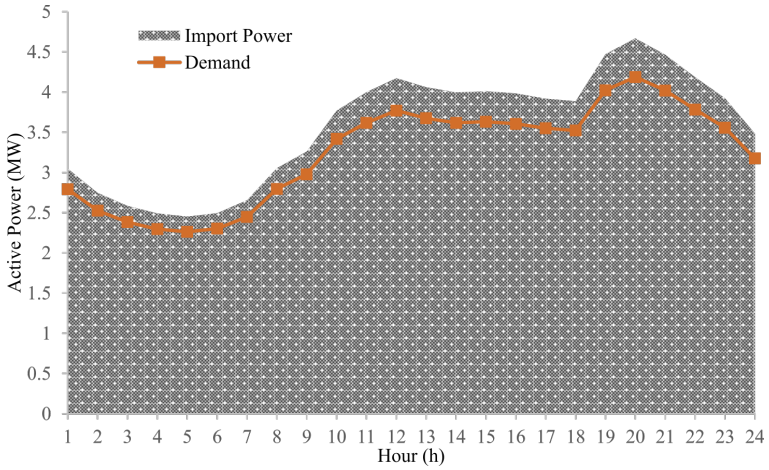

Figure 4.7: Energy mix of the base case

4.3.2 CB only case

With the inclusion of capacitor banks (CB only case), voltage deviations could be partly managed since there are now reactive power sources within the system. Voltage profiles now respect the limits as it can be seen in Figure 4.8. In fact, only the lower limit constraint is active. SCBs have a considerable impact in voltage deviations since the resistance and reactance values, of the considered grid, are not too far apart.

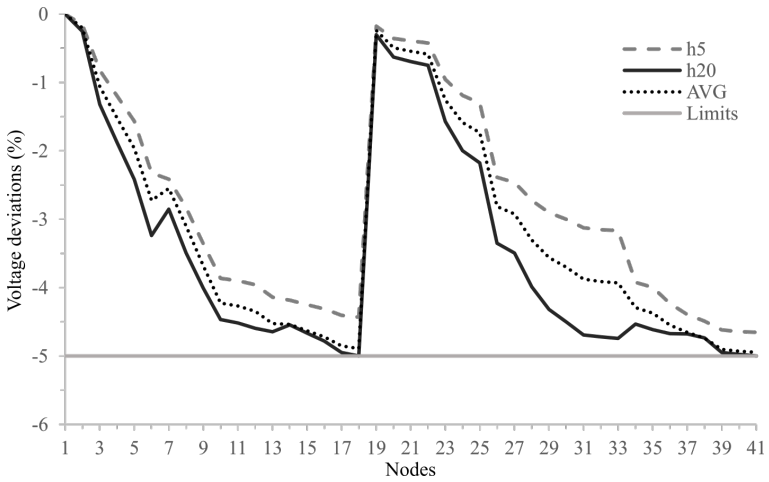

Figure 4.8: Average voltage deviations at each node for the CB only case

By including capacitor banks, reactive power demand can be met locally which diminishes the apparent power flow in lines. For this reason, losses have decreased, as it can be seen in Table 4.3, compared with the base case, since they depend on active and reactive power flows as stated in Equations (3.19) and (3.20). Since the amount of both active and reactive power required in the system, especially the latter one, is lower, the average substation power factor is improved to 0.99. As a result, system total cost is reduced by 2.6% and most importantly, voltage deviations are improved on average by 45.1% respecting the imposed limits. Since, in this case, only the

upstream grid and SCBs are considered, costs only concern imported power and its respective emissions, as in the first case. In addition, this case also follows the classic grid active power flow. However, bus 7 has a higher voltage than bus 6 (in the same branch) because it is mainly exporting reactive power to upstream buses.

The energy mix in this case, presented in Figure 4.9, is very similar to the previous one. The difference between the two illustrations is perceptible, where in Figure 4.9 power production is closer to the demand, than that in Figure 4.7. This reveals the significant reduction in power losses due to SCBs, as it can be observed in Table 4.3.

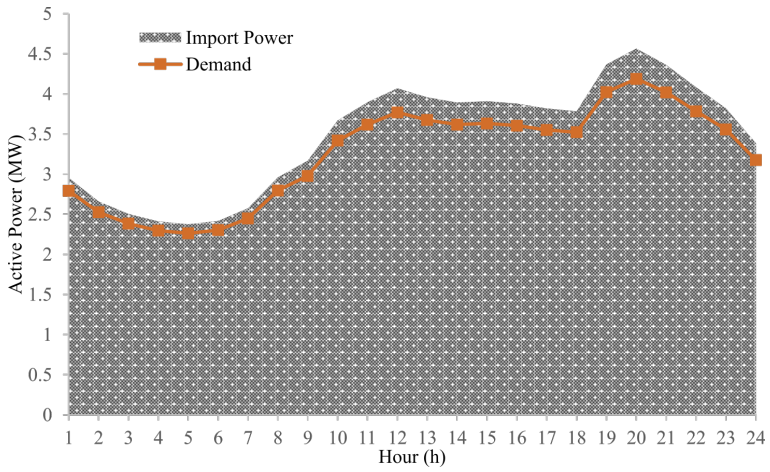

Figure 4.9: Energy mix of the CB only case

4.3.3 No ESS case

In this case, a system with large scale RES is considered together with SCBs. Comparing with both the Base case and CB only cases, voltage profiles, losses and cost have improved significantly.

As a matter of fact, average voltage profiles with the inclusion of RES vary between the upper bound during hour 24 and the lower bound during hour 20, as it can be observed in Figure 4.10. Moreover, the lower bound hour is equal to the previous cases since demand is at its peak and import power is required. However, upper bound hour changes, in this case, because demand is high on hour 24, compared to hour 5 as seen in Figure 4.11, and it is met using wind power production which is located at far end buses, as stated in Table 4.1. As a result, voltages at these buses increase so that they can export power to upstream buses. This is especially perceptible in bus 14 which delivers power to local demand, downstream and upstream buses in both hour 20 and 24.

It is worth noting that, even if the power factor at the substation is defaulted to 0.8, in reality, the power factor in this case is 0.91 on average.

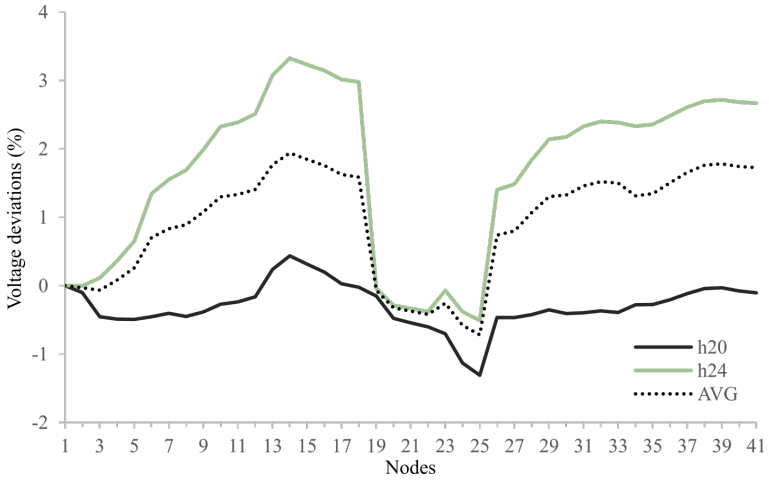

Figure 4.10: Average voltage deviations at each node for the No ESS case

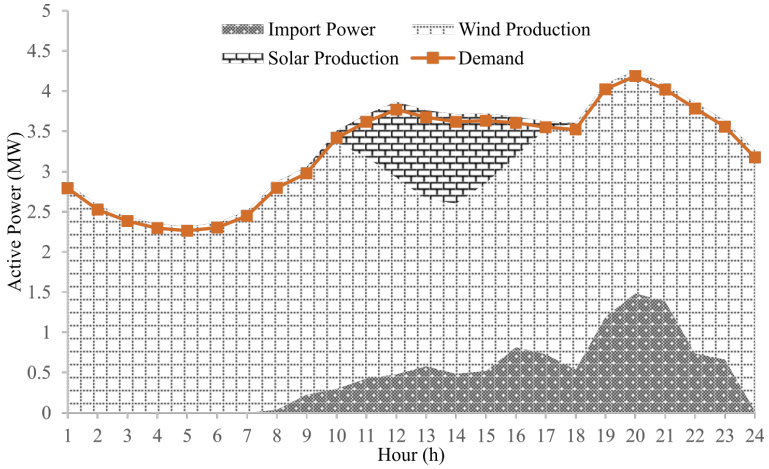

Figure 4.11: Energy mix of the No ESS case

With the inclusion of large scale RES, the weight of import is reduced significantly, as expected. In fact, import energy, in this case, represents 13.3% of total power production while RES share is 86.6% (Wind 80% and PV 6.6%). In Table 4.3, it is possible to observe that by including RES, costs have decreased significantly, comparing with the base case, and so did losses. It is important to refer that despite a high penetration level of RES, there is still curtailed power in wind and solar power production. This can be partly explain as follows. In the current work, demand growth is not accounted for; the base case load is maintained throughout the analysis. However, the optimal solution of the distributed energy resources (DER) in [33] considers yearly demand growth over a three-year horizon. This means that the total DER capacities could be overdimensioned for the base case, as the results show here (i.e curtailment of RES power production).

In fact, curtailed power in wind power production is 17.8% and in solar power production it is 10%, as can be seen in Figure 4.12. Note that, in the referred figure, "P_W" and "P_PV" represent the maximum wind and solar power production outputs, respectively, while "W_real" and "PV_real" stand for the actual power produced from these sources. The majority of wind power

curtailment happens during early hours, as seen in Figure 4.12, because production surpasses demand. As solar production is more expensive than wind and is only located at buses 32 and 38, it is curtailed even when import is required to meet demand. This occurs because increasing solar power production would affect system losses, increasing the overall cost.

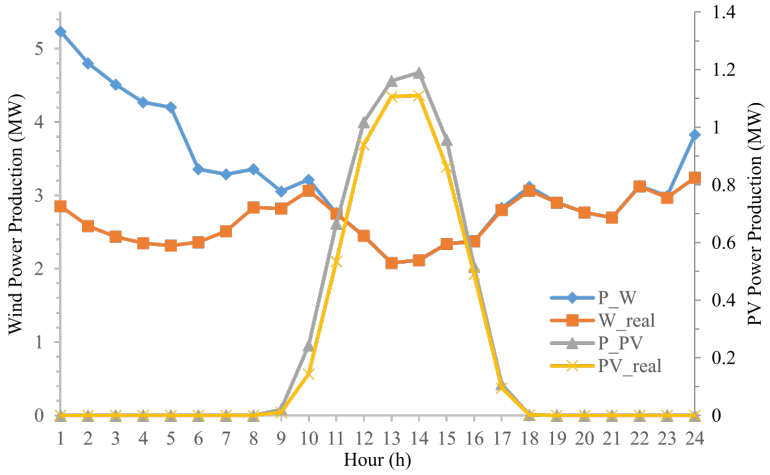

Figure 4.12: Actual DG production vs DG potential in the No ESS case

4.3.4 EFF 0.9 case

Considering all technologies connected to the grid (DGs, ESSs and SCBs), there is a complete change on the voltage profile, as seen in Figure 4.13. Similar to the No ESS case, as DGs are included, voltage profiles are altered so that power flows can now occur from downstream to upstream. Additionally, because of ESS, there is an inversion of lower and upper voltage deviation hours. In fact, voltage deviations are higher for high demand hours (hour 20) because, as it can be analysed in Figure 4.14, ESSs act like a demand early in the day while they are charging. This means total demand is now higher for hours 1 until 5. A detailed analysis reveals that hour 19 had the highest voltage deviation in bus 41 instead of at peak demand of hour 20, because in hour 19 there is higher wind production that goes upstream (bus 39). However, hour 20 has higher average voltage deviations because of high ESS discharge in that period.

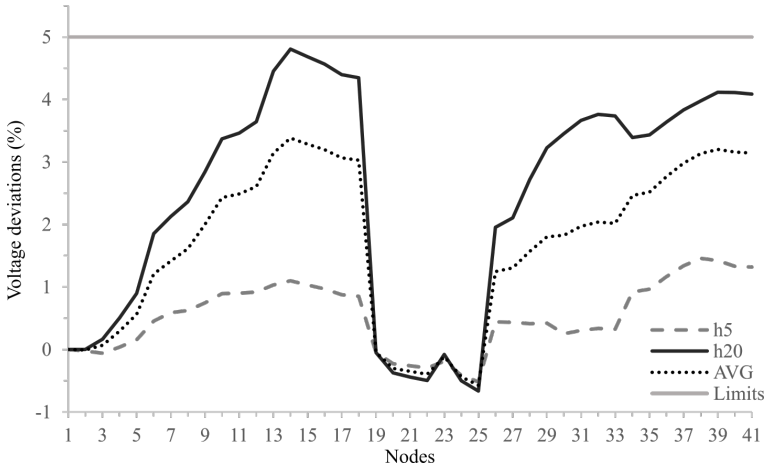

Figure 4.13: Average voltage deviations at each node for the EFF 0.9 case

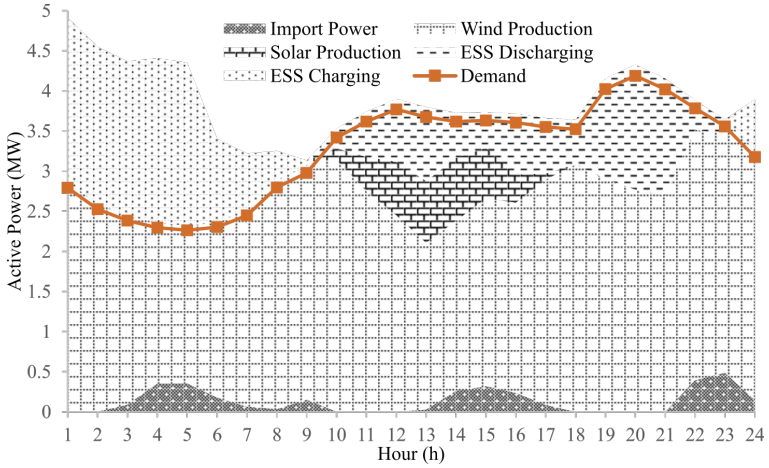

Figure 4.14: Energy mix of the EFF 0.9 case

Additionally, bus 14, 32 and 38 have the highest installed capacities of DGs and ESSs, and each one of these buses belongs to a different branch of the grid, and are located near the end of the corresponding branch. As it can be observed in Figure 4.13, buses 14 and 32 have the highest positive deviation (of the corresponding branch), which means they dispatch energy for the surrounding buses and loads, because production surpasses the local demand. As for bus 38, it has another bus with DGs in the same branch (bus 39), it dispatches power to upstream buses since demand at node 39, 40 and 41 are met by the local production at bus 39. Note that the situation at bus 38 only occurs because local production at bus 39 surpasses local demand. The same situation happens on bus 7 because of the existence of power production in downstream buses.

It can be observed in Figure 4.14 that, during valley hours, the system uses the excess wind power production and a slight import of power to charge the energy storage systems, since prices are low and it is beneficial in terms of losses reduction. When wind power production diminishes, ESSs begin to discharge, and together with solar production, the demand is met. Furthermore, because solar power production is more expensive, regarding tariffs, than ESSs and wind power

production, a curtailment of solar power is observed (34.6%). This happens since discharging the stored energy is cheaper, because it originates from wind type DGs. In fact, wind power curtailment is only 2.5%. Curtailed and actual power production are conveniently shown in Figure 4.15.

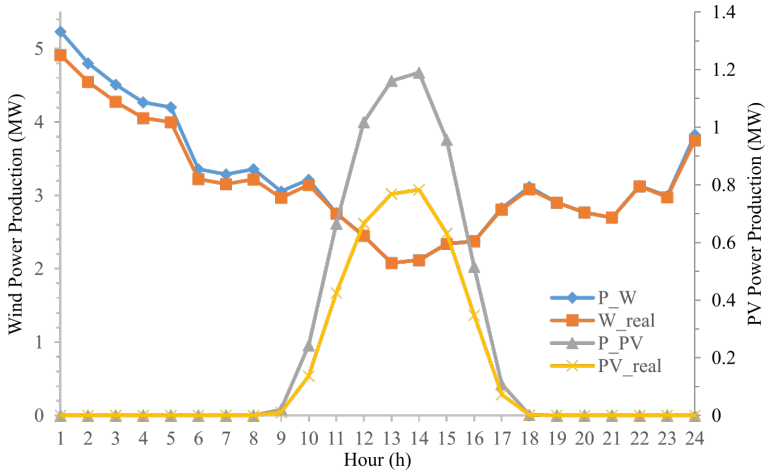

Figure 4.15: Actual DG production vs DG potential in the EFF 0.9 case

Despite being more expensive, solar PVs must be used, since later in the day, there will not be any and power import will be more expensive. In other words, a total curtailment of solar power would be counterproductive since ESSs can be used more efficiently later in the day, and also because it would mean curtailing a valuable resource totally dependent on the time of day. To compensate the lack of solar power during peak hours, when electricity prices are higher, ESSs can be used to partially meet demand, avoiding the need to import energy at high prices.

In order to analyse if the amount of energy charged is equal to the amount of energy discharged, the area related to charging must be multiplied by ESS charging efficiency, and the discharging area divided by the discharging efficiency. This is necessary because the charging area shown in Figure 4.14 represents the total energy absorbed by ESSs (including ESS losses) while the discharging area represents energy injected into the system (after discharging losses).

In this case, cost is reduced by 69% and losses by 70% compared to the base case. Moreover, RES penetration reached 96.1% (Wind 91.5% and PV 4.6%) while import is only 3.9%. In table 4.3, it can be observed that the majority of costs concerns RES operation and emissions.

As stated before, since DGs are present in the system and as they have reactive support capability, less reactive power is imported from the substation. Additionally, active power required from the transmission grid is also low. As a result, the power factor at the substation, in this case, is 0.9 on average.

Comparing No ESS and EFF 0.9 cases, it is possible to conclude that including ESSs diminishes costs significantly (20%) and increases RES penetration by 9.5%, despite curtailing more solar power production in EFF 0.9 case.

4.3.5 EFF 0.8 case

Considering ESSs with lower efficiencies, in this case 80% charging/discharging efficiency, leads to a decrease in the utilization of these systems, since it would require more energy to use them efficiently. This affects voltage profiles slightly which are now on average, lower than on EFF 0.9 case (0.09% below the average in EFF 0.9). However, analysing both hour 5 and 20 in Figure 4.16, they present higher voltage deviation in this case than for the same period in case EFF 0.9. The average is lower because there are less high discharge periods during the day, as can be seen in Figure 4.17. This means voltage deviations will be lower. In effect, comparing both Figures 4.14 and 4.17, it possible to conclude the discharging area is smaller in case EFF 0.8 than in EFF 0.9.

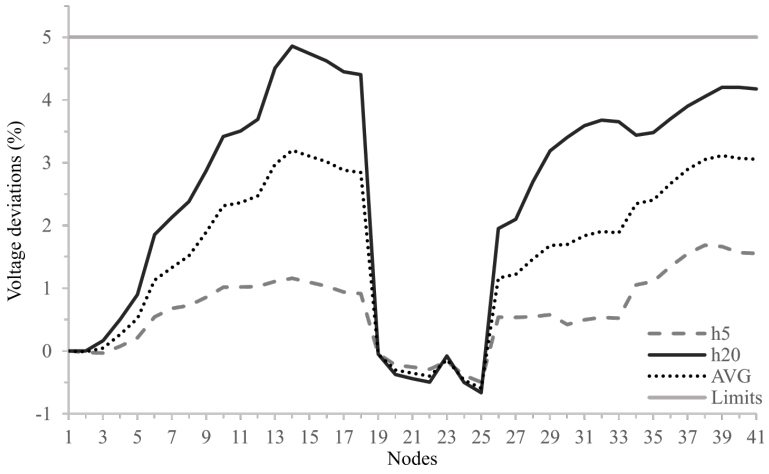

Figure 4.16: Average voltage deviations at each node for the EFF 0.8 case

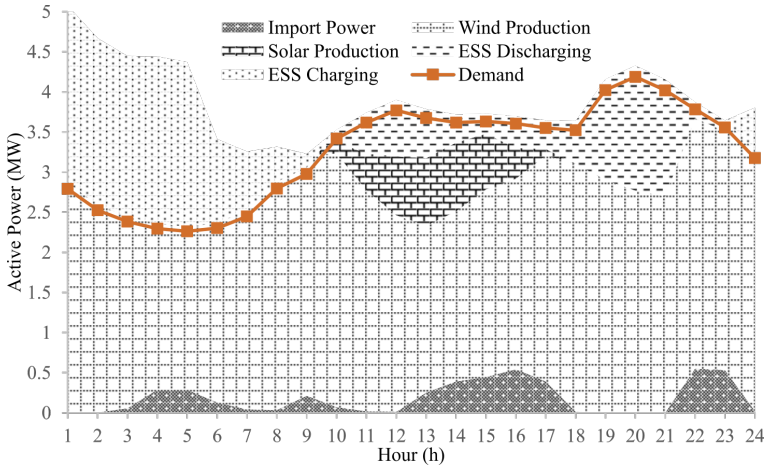

Figure 4.17: Energy mix of the EFF 0.8 case

When ESS efficiency is reduced, the otherwise curtailed solar production must now be used to compensate, since stored energy will be needed later in the day. In fact, curtailed solar power production reduced to 28.6%. Moreover, to overcome the increase in charging losses, less wind

power is curtailed in the beginning of the day, reducing curtailed wind power to 1.4%. In fact, it is possible to observe in Figure 4.18 that, in this case RES dispatches more power than in the EFF 0.9 case. However, because ESS efficiency is lower, the amount of "useful" charge and discharge power is reduced. As a result, ESS discharging periods are reduced, so that stored power can be more efficiently used when electricity prices are higher. This means more imported power is required, especially between hours 12 and 18, reducing RES share to 94.9% (Wind 90% and PV 4.9%) and improving imported power share to 5.1%.

In this case, the actual average power factor at the substation level is 0.89.

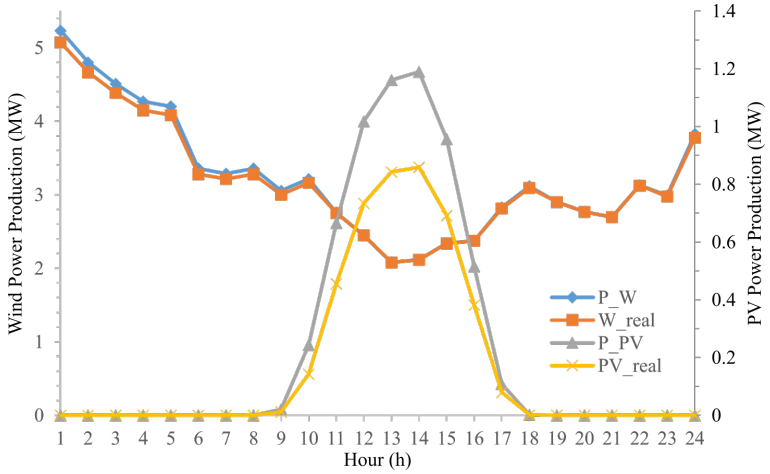

Figure 4.18: Actual DG production vs DG potential in the EFF 0.8 case

4.3.6 EFF 0.7 case

Further reducing ESS efficiency means that average voltage deviations will be lower than on EFF 0.8 case. In this case, average voltage deviations are closer to the nominal value. This is, 0.19% below the average in EFF 0.9 case.

As referred in the previous case, despite observing a positive shift in the maximum and minimum voltage deviation hours, as seen in Figure 4.19, the average value is lower because there are less periods where ESS is discharging. Moreover, the minimum voltage deviation now occurs at hour 16 instead of at hour 5 as in EFF 0.9 and 0.8 cases. In this case, at hour 16, there is little discharge from ESSs (Figure 4.20), compared with the other cases. This means that more power is going to be required from the transmission grid, since DGs are already producing at their limits (Figure 4.21). As a result, since there is less power dispatched from downstream buses and because import power is going to supply loads close to the substation, voltage deviations are slightly lower.

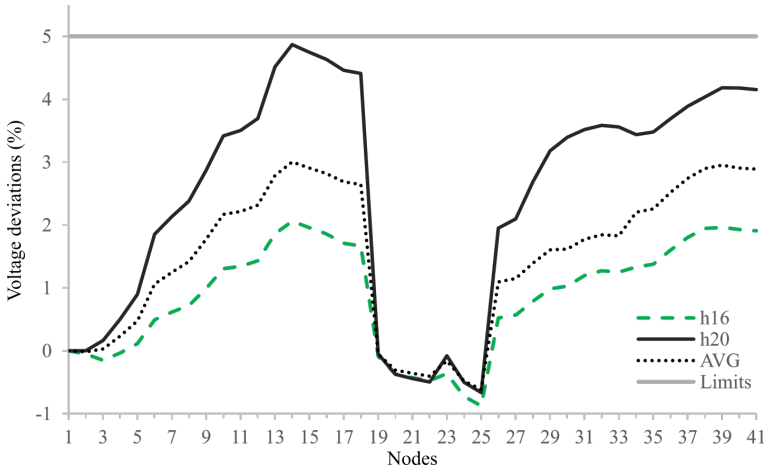

Figure 4.19: Average voltage deviations at each node for the EFF 0.7 case

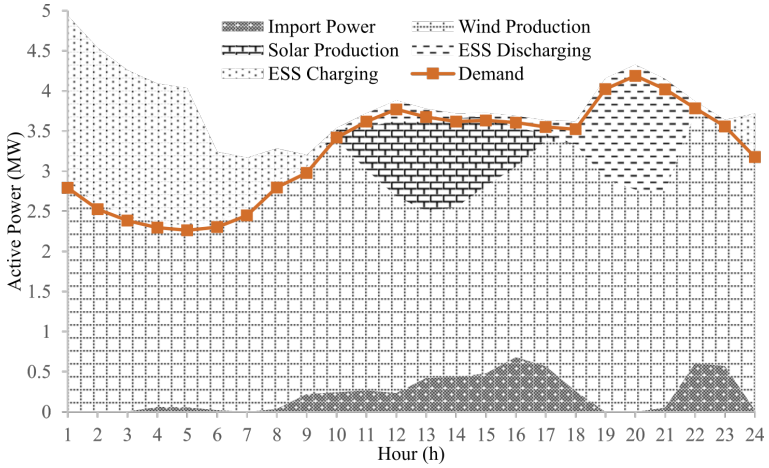

Figure 4.20: Energy mix of the EFF 0.7 case

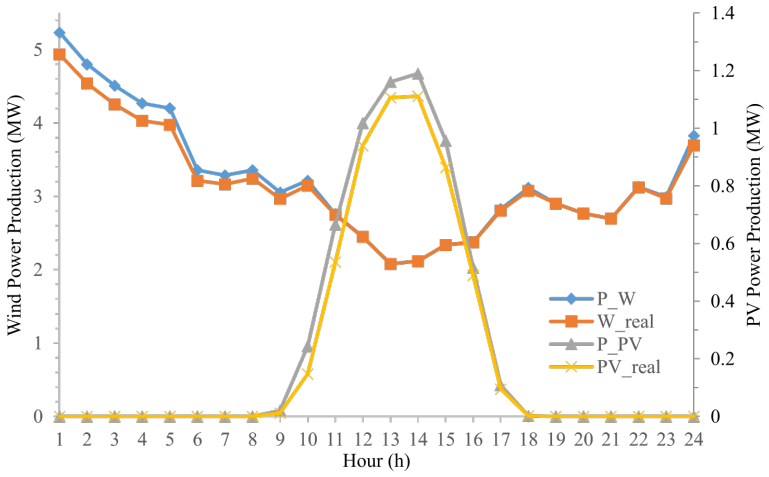

Figure 4.21: Actual DG production vs DG potential in the EFF 0.7 case

A more detailed analysis also demonstrates that, with 70% ESS efficiency, wind power would be slightly curtailed early in the day, improving the amount of wind power curtailment to 2.6%, while solar power curtailment is reduced to 9.9% since it must be used so that ESSs can discharge later in the day. Furthermore, because ESS efficiency is lower than the other cases, there is little import power early in the day since wind power production is used more efficiently to meet demand instead of charging ESS. This means, ESSs will have less power available for discharge, hence their use is going to be limited.

In Table 4.3, both cases with altered efficiencies show higher costs of operation and emissions, because of increased use of DGs. At the same time, more import power cost, and respective emissions are noticed since stored energy is intended to be used later in the day when electricity price is higher. On the other hand, losses decreased slightly when compared to EFF 0.9 case since less discharge power is used during the day.

Despite low ESS efficiency, RES share reached 93.9% (Wind 87.7% and PV 6.2%) while import power represented 6.1% of total power production.

It is important to note that, the actual substation power factor was 0.9, on average.

4.3.7 No limit Q case

When excluding the reactive power limits, by removing constraints (3.35), (3.36) and (3.37), active power export is now allowed, which means import prices can be negative (i.e. excess power can be sold to the grid).

Average voltage profiles are slightly improved when compared to EFF 0.9 case, since there is active power export at the same time as reactive power import. However, voltage deviations are highly variable between hours 5 and 21, as it can be seen in Figure 4.22. In fact, upper bound hour 21 presents higher voltage deviations, since there is a high level of power being exported to the substation, originated from RESs and ESSs located near the end of the grid. On the other hand, as wind power is mainly used to charge ESS on hour 5, import power is best directed to meet demand, hence voltage deviations are lower.

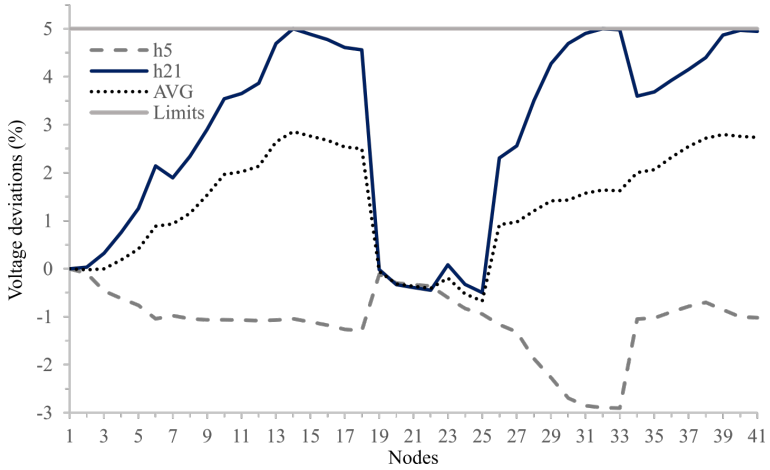

Figure 4.22: Average voltage deviations at each node for the No limit Q case

Additionally, hour 21 has the highest positive voltage deviations (instead of hour 20) since demand is lower, and both bus 14 and 32 are at their maximum deviations, because they will mainly dispatch power to upstream buses. This means that, at bus 6 and 10, voltage deviations will be higher, since they do not diminish as much as in hour 20 from bus 32 to 6 or from 14 to 10. Additionally, bus 40 is discharging for the surrounding buses, offsetting deviations in hour 21. The reader might notice that, at hour 21, voltage deviation at bus 6 is higher than at bus 7, despite active power flows from bus 7 to bus 6 (line 6). This happens because, contrary to CB only case, bus 7 is now exporting reactive power to downstream buses while still receiving reactive power from bus 6.

In terms of cost, because excess energy is sold to the upstream grid, this case presents the lowest cost, as demonstrated in Table 4.3. However, losses increase because DG nodes are on the far end of the grid, and in order to export active power, it must pass through several lines until it reaches the substation, thereby increasing losses (when compared with EFF 0.9 case). Nevertheless, losses are still lower than in the Base case.

In Figure 4.23, it is possible to observe the several cycles of operation. For example, early in the day, it is preferable to sell part of the wind power over using it totally to meet demand and charge the ESSs. On hour 5, when electricity prices are low, the system uses import to store the maximum amount of power so that it can discharge when price is at its maximum, hence diminishing total costs through high level export to the transmission grid. In this figure, the representation of export power is considered to a negative area because it eases loss analysis as stated in previous cases. In fact, from hour 19 to 21 losses reach their maximum, as expect, due to high level power flow from ESSs and DGs, in downstream buses, to the transmission grid with the intention of exporting when prices are higher. Because DG and ESS have low operation costs, compared to the price of importing power, and as export is now allowed, there is no curtailment of RES. Despite increasing losses in low demand hours, for example, the fact is the cost of losses can be compensated with the possible income generated from selling excess power, since it originates from wind power production, cheap energy sources.

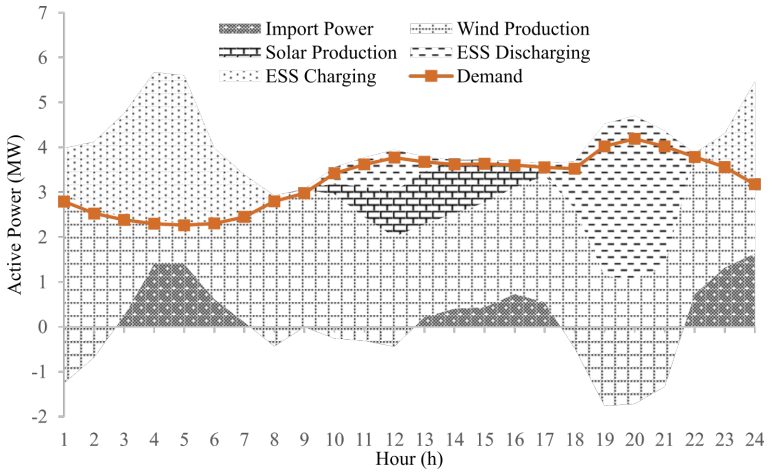

Figure 4.23: Energy mix of the No limit Q case

4.4 Specific Analysis

To further illustrate the behaviour of the proposed operation model under specific scenarios, with high power production variability and high demand, additional cases are also considered under EFF 0.9 case assumptions.

Note that the following cases are already taken into account in EFF 0.9 case. However, as EFF 0.9 case represents the average of 1000 different scenarios, specific situations can be difficult to analyse in that form. Each additional case contains an analysis of the effect of ESS in the system, under specific demand, wind and solar power production scenarios:

- Case A: high peak demand (d6) and high RES variability (w9 and pv9) scenarios;
- Case B: high average demand (d3) and high RES production (w4 and pv2) scenarios;
- Case C: high average demand (d3), low wind power production (w3) and high solar power (pv2) production scenarios.

Cost and losses for the following cases are presented in Table 4.4.

Table 4.4: Relevant system variables for each additional case

Case	Case A	Case B	Case C
Operation Cost (€)			
DG	1638.28	1938.28	1768.71
ESS	57.41	59.77	56.25
Cost import [€]	629.60	0.00	611.99
Cost unserved [€]	0.00	0.00	0.00
Cost of Emissions [€]			
DG	13.63	16.15	14.82
Substation	25.46	0.00	28.54
Total Cost [€]	2364.39	2014.20	2480.32
Average Losses			
PL [MW]	0.09	0.11	0.10
QL [MVAr]	0.07	0.09	0.08

4.4.1 Case A: High peak demand, high RES variability

In this case, the selected demand scenario is scenario 6 because it has the highest values of peak demand, together with highly variable wind and solar production scenarios. The most variable wind and solar production scenarios are scenario 9, on both production sources.

The selected scenarios are conveniently shown Figure 4.24.

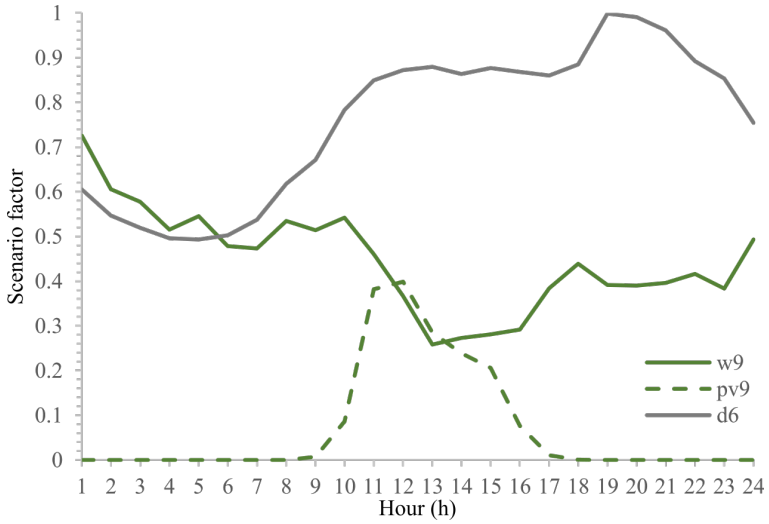

Figure 4.24: Scenarios used in Case A

These scenarios are chosen because, during high demand periods, there is a sudden break in both wind and solar power production, that begins at hour 10 for wind and overlaps with solar power production at hour 12. Furthermore, in three consecutive hours, wind power production reduces by 52.3% (from hour 10 to 13) and overlaps with a 28.4% decrease in solar power production from hour 12 to 13. Solar power production continues to decrease after hour 13, until it reaches 0 at hour 18.

In Figure 4.25, it is possible to observe that, when there is a sudden break in wind and solar power productions, ESS discharges to cope with that. When electricity prices decrease, the system imports power since stored energy is more efficiently used later in the day when prices reach their maximum limits. However, if not for ESS, the required import power would begin immediately after power generation loss which coincides with high electricity prices, increasing costs.

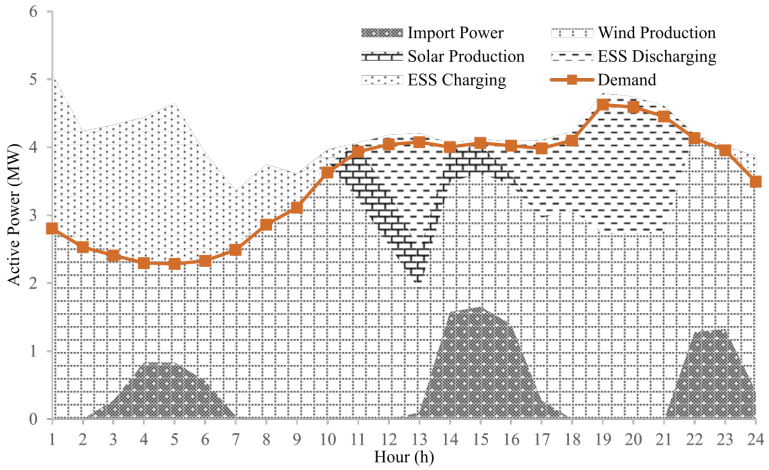

Figure 4.25: Energy mix of Case A

Through this technology, demand is met instantaneously with little change to voltage profiles,

as it can be seen in Figure 4.26 for hour 10 (before break in production) and hour 13 (during peak ESS discharge). The most notorious changes in voltage profiles can be observed in bus 14 and 32, because, at hour 13, these buses are discharging to the surrounding ones, affecting voltage profiles. Comparing both of these periods, it is also possible to conclude that voltage profiles improve in hour 13 for downstream buses from bus 35, because wind power production at bus 39 diminished and ESS, installed at bus 40, discharge can meet local demand. This way, line 39 has no power flow, which is not true on hour 10 since ESSs are charging using RES power.

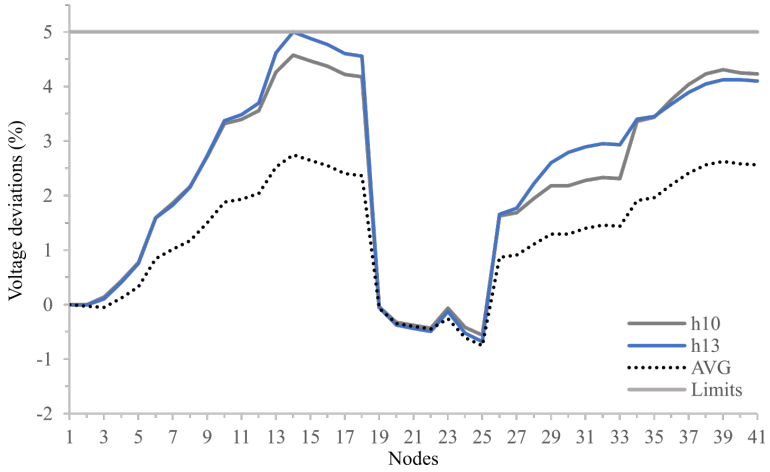

Figure 4.26: Average voltage deviations at each node for Case A

4.4.2 Case B: High average demand, high RES Production

For this case the scenarios selected for the specific analysis are demand scenario 3, because it has the highest average demand for the 24 h period, wind and solar power production scenarios 4 and 2, respectively, due to their high average profile. The considered scenarios can be seen in detail in Figure 4.27.

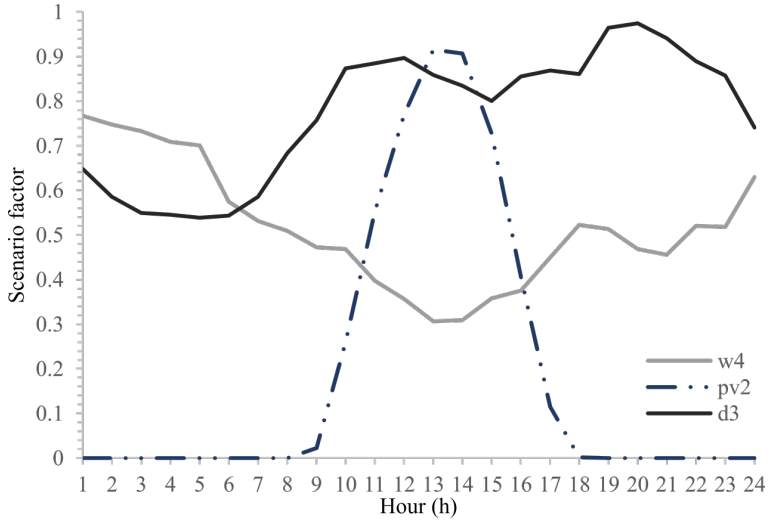

Figure 4.27: Scenarios used in Case B

In Figure 4.28, it is possible to conclude that demand is supplied using only RES and ESS. This means RES share reaches 100%, requiring no import power from the transmission grid. Despite high wind and solar power productions, there is still 42% solar power curtailment, since discharging ESS is cheaper.

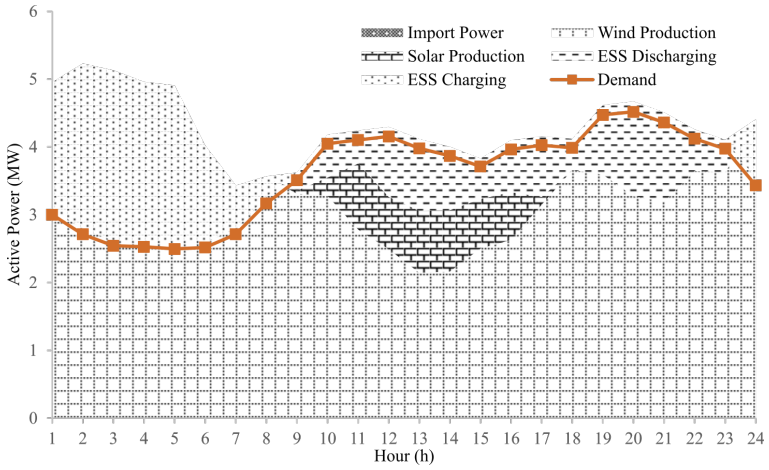

Figure 4.28: Energy mix of Case B

Similar to the previous cases, ESS and solar power production are used to compensate the loss of wind power production. For example, when wind power diminishes after hour 9, ESS is dispatched and when possible solar power is also utilized.

Compared with No ESS case, this case allows for a significant cost reduction despite increasing losses, through 100% RES integration. In fact, active and reactive losses are 0.11 and 0.09 MW while total costs are 2014.20 € and they only concern DG and ESS operation and emission costs, as demonstrated in Table 4.4.

Furthermore, since there is no power imported from the upstream grid, generation is concentrated in far end buses. This affects voltage profiles, which are higher than that of the EFF 0.9 case. In Figure 4.29, average voltage deviation profiles for both cases are shown.

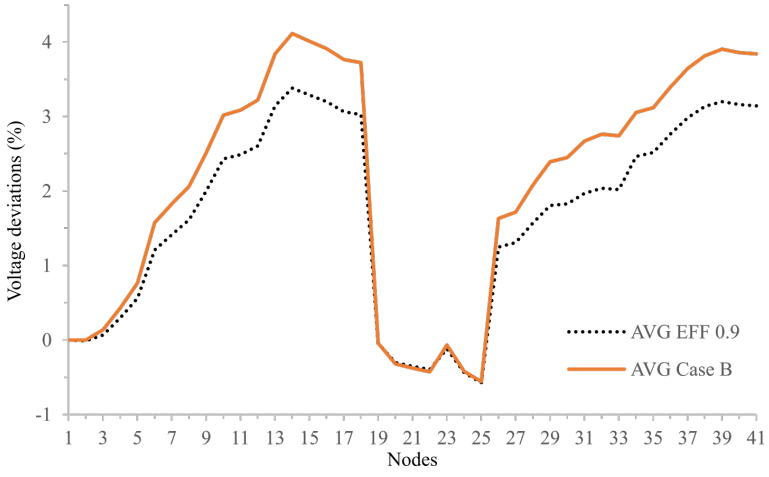

Figure 4.29: Average voltage deviations of Case B and EFF 0.9

4.4.3 Case C: High average demand, low wind Production, high solar production

For high average demand (scenario 3) with low average wind power production (scenario 3) and high solar power production (scenario 2), it is possible to observe in Figure 4.30 that because, in early day, wind power production is low, the system uses import power at low prices to meet the majority of demand, while wind power production is used to charge the ESSs. In this case there is no generation curtailment since wind power production is low and must be absorbed so that cost can be even further reduced later in the day, and because all available solar power production must be used in order to minimize ESS discharge during mid-day periods.

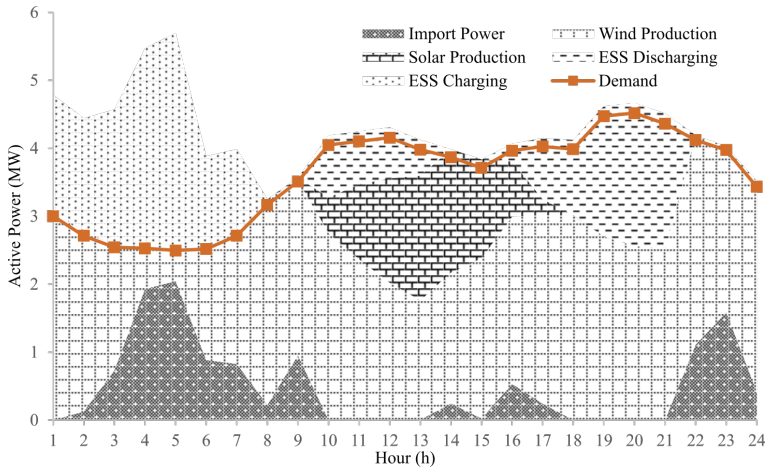

Figure 4.30: Energy mix of Case C

In average terms, voltage profiles improve when compared to EFF 0.9 case (closer to the nominal voltage), however because of high variability in power flows voltage profile are highly variable in this case.

4.5 Problem Complexity

As it is possible to observe in Table 4.5 the number of equations and variables involved in one of the most complex cases (EFF 0.9), is very high, even considering the mathematical approximations in Chapter 3 and the scenario reduction explained in this Chapter.

Table 4.5: Problem complexity of the EFF 0.9 case

Non zero elements	96 192 014
Single equations	32 068 088
Single variables	33 552 008

4.6 Chapter Summary

This work has proposed a new stochastic MILP model that aims to ensure a more efficient utilization of large scale variable renewables at distribution levels. The results show that the integration of ESS together with reactive power sources could sufficiently cope with the variability of RESs, reducing losses and cost, while improving voltage profiles in the system.

ESSs have increased renewable energy penetration significantly, since excess wind power could be stored and used later, instead of being curtailed. This way, the integration of ESSs allow a more efficient use of renewable energy sources, which are almost emission-free power sources. As a result, this is reflected in the overall cost reduction. In fact, RESs can represent 100% of the total electricity consumption. A good planning of the location and capacity of RES is also required.

As demonstrated in this study, with the integration of RESs, ESSs and SCBs in the right locations, active power losses in the EFF 0.9 case could be reduced by 70% on average, and total cost in the same case by 69%.

Furthermore, the proposed model considerably improves voltage profiles in the system, as it is possible to observe in Figure 4.31. In the referred figure, for different ESS efficiencies, only EFF 0.9 is presented, since voltage deviations do not vary significantly between those cases. Note that, including ESSs further increased the average voltage deviations. This happens since more power is dispatched from downstream buses.

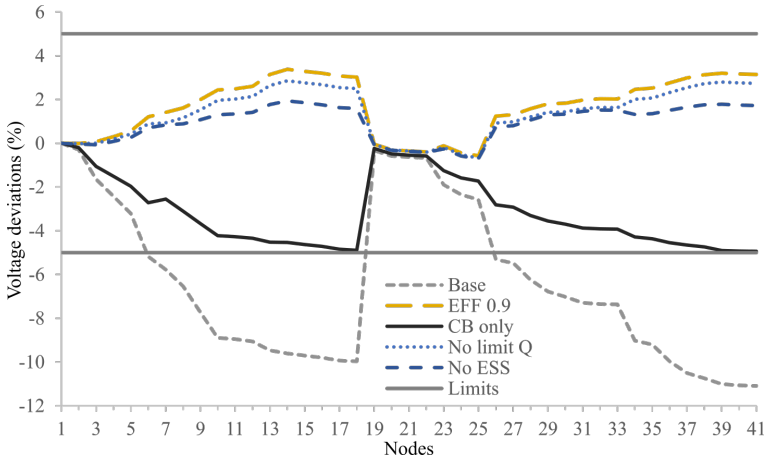

Figure 4.31: Comparison of voltage profiles of the cases presented in Table 4.3

Chapter 5

Conclusions and Future Works

5.1 Conclusions

This work has proposed a new stochastic MILP model that aims to ensure a more efficient utilization of variable renewables at distribution levels, using ESSs and SCBs. The proposed operational model is formulated in a stochastic environment, accounting for both variability and uncertainty pertaining to demand, wind and solar power productions. This is achieved by considering 10 different scenarios for each. Such considerations allow a more realistic analysis, under various operational conditions. The objective function is to minimize the sum of expected costs of operation, unserved power, and emissions while meeting the most relevant technical and economic constraints.

The operational analysis has been carried out on an IEEE 41-bus network system, particularly covering the effects of ESSs and SCBs on the system performance in terms of costs, losses, voltages and energy mix.

The results show that the deployment of ESSs together with reactive power sources can effectively cope with the variability of RESs, reducing losses and cost, while improving voltage profiles. It has been demonstrated that deploying ESSs and SCBs improve voltage profiles considerably, which in turn contributes to an increased voltage stability margin, essential for a secure operation of the system.

The variation of ESS efficiency does not have significant impact on voltage deviations, however it affects, as expected, the amount of RES energy stored and injected into the power system. Through ESS, renewable energy penetration increased significantly, since excess wind power could be stored and used later, instead of being curtailed. It is important to note that the deployment of ESS allows a more efficient use of renewable energy sources, which are almost emission-free power sources, and this is reflected in the cost. However, for lower efficiencies, the share of RES in the energy mix can me misleading, since more power has to be absorbed to charge the same amount as in higher efficiencies. This also affects discharging, since for the same discharged power, as in higher efficiencies, there is more power required from the ESS, which means energy

stored will be depleted faster. Therefore, for lower ESS efficiencies, these systems are going to be less used, and more RES power is wasted in charging and discharging losses, which is not ideal.

As demonstrated for high and low wind power production (Case B and C presented in section 4.4), ESSs can be used in different ways, always minimizing total system cost. For high wind power production, ESSs store excess wind power, which would have been otherwise curtailed; So it can minimize cost by maximizing the integration of cheaper energy when price is higher. However, when RES power production is low, the system uses import to meet demand so it can store cheaper wind power to use when prices, and demand, are higher.

In average terms, RESs can represent 96% of the total power production. A good planning of the location and capacity of RES is also required, since this will affect losses depending on the locations, sizes as well as the profile of wind and solar outputs. As demonstrated in this study, with the integration of RESs, ESSs and SCBs in the right locations, active power losses in the EFF 0.9 case could be slashed by 70% on average, and total cost in the same case by 69%.

5.2 Future Works

The objective function of the proposed model is to minimize total system costs. To model ESS costs, a small value per MW discharged has been considered. This cost models the deterioration of the ESS during the charging and discharging process. However, in this study, for different ESS efficiencies, the discharging cost remains the same. In order to incentivise the use of high efficiency batteries, different discharging costs could be associated with efficiencies. This way, ESS efficiency could be directly modelled in the objective function. This would involve studying different ESS technologies in detail, in particular the number of cycles it can do in a lifetime, and what materials are required for their construction. This last characteristic is important, since minimizing environmental impact should also be a concern.

With the integration of ESS in distribution systems with large scale RES installed, it is possible to manage the variability and uncertainty that characterised these systems. In fact, excess variable RES production can be stored and used when the distribution system operator so desires. This means that, to a certain level, depending on the installed capacity of ESS, variable RES production can no longer be defined as totally non-dispatchable. Therefore, it can be directly integrated into the market, without the need for tariffs schemes. However, this must be thoroughly studied, since benefiting RES production is a central part of a "carbon-free" future.

5.3 Works Resulting from This Dissertation

As part of the main contributions, this dissertation has led to two scientific papers, one of which can be found appended here (see Appendix C) and the other is under review for publication in a journal:

- M.P.S. Pereira, D.Z. Fitiwi, S.F. Santos, J.P.S. Catalão, "Stochastic Analysis of Operating Distribution Network Featuring Large-scale Distributed Energy Resources", *IEEE Trans. Sust. Energy* (Submitted);

- M.P.S. Pereira, D.Z. Fitiwi, S.F. Santos, J.P.S. Catalão, "Managing RES uncertainty and stability issues in distribution systems via energy storage systems and switchable reactive power sources", in: *Proceedings of the 17th IEEE International Conference on Environment and Electrical Engineering — EEEIC 2017*, Milan, Italy, 6-9 June, 2017 (Accepted for publication).

Appendix A

Flow Based Loses

The demonstration and assumptions made to reach equations (3.19) and (3.20) are presented here. Squaring both sides of each power flow equation in (3.10) and (3.11), we get:

$$\begin{aligned}\frac{P_l^2}{V_{nom}^2} \approx\ & [(\Delta V_i - \Delta V_j)g_l]^2 \\ & - 2 * g_l V_{nom} b_l \theta_l (\Delta V_i - \Delta V_j) \\ & + (V_{nom} b_l \theta_l)^2\end{aligned} \tag{A.1}$$

$$\begin{aligned}\frac{Q_l^2}{V_{nom}^2} \approx\ & [(\Delta V_i - \Delta V_j)b_l]^2 \\ & + 2 * b_l V_{nom} g_l \theta_l (\Delta V_i - \Delta V_j) \\ & + (V_{nom} g_l \theta_l)^2\end{aligned} \tag{A.2}$$

Considering that variables, θ_l, ΔV_i and ΔV_j are very small, equations (A.1) and (A.2) can be simplified as:

$$\frac{P_l^2}{V_{nom}^2} \approx (V_{nom} b_l \theta_l)^2 \tag{A.3}$$

$$\frac{Q_l^2}{V_{nom}^2} \approx (V_{nom} g_l \theta_l)^2 \tag{A.4}$$

Then, multiplying (A.3) and (A.4) by r_l and summing both parts:

$$r_l \left(\frac{P_l}{V_{nom}}\right)^2 + r_l \left(\frac{Q_l}{V_{nom}}\right)^2 \approx r_l (V_{nom} b_l \theta_l)^2 + r_l (V_{nom} g_l \theta_l)^2 \tag{A.5}$$

After rearranging (A.5), we get:

$$r_l \frac{P_l^2 + Q_l^2}{V_{nom}^2} \approx g_l (V_{nom} \theta_l)^2 r_l * \left(\frac{b_l^2}{g_l} + g_l\right) \tag{A.6}$$

since $r_l * \left(\frac{b_l^2}{g_l} + g_l\right) = 1$, then (A.6) can be reduced to:

$$r_l \frac{P_l^2 + Q_l^2}{V_{nom}^2} \approx g_l (V_{nom}\theta_l)^2 \tag{A.7}$$

By analyzing (3.17) and (A.7), the derivation presented is proved. Reactive flow based losses (3.18) are derived in a similar way. By multiplying (A.3) and (A.4) by the reactance of the line x_l instead of the resistance, the following equation is obtained:

$$x_l \frac{P_l^2 + Q_l^2}{V_{nom}^2} \approx -b_l (V_{nom}\theta_l)^2 x_l * \left(\frac{g_l^2}{-b_l} - b_l\right) \tag{A.8}$$

Note that, $x_l * \left(\frac{g_l^2}{-b_l} - b_l\right) = 1$. Then, (A.8) can be reduced to:

$$x_l \frac{P_l^2 + Q_l^2}{V_{nom}^2} \approx -b_l (V_{nom}\theta_l)^2 \tag{A.9}$$

Analyzing (3.18) and (A.9), it can be observed that both represent the same expression, also proving the derivation.

Appendix B

IEEE 41 Bus Distribution System

Table B.1: Parameters of the IEEE 41 Bus Distribution system

Lines	FROM	TO	R	X	S^{max}	Node	DemP	DemQ
line1	1	2	0.0992	0.047	6.986	2	100	60
line2	2	3	0.493	0.2511	6.986	3	90	40
line3	3	4	0.366	0.1864	6.986	4	120	80
line4	4	5	0.3811	0.1941	6.986	5	60	30
line5	5	6	0.819	0.707	6.986	6	60	20
line6	6	7	0.1872	0.6188	6.986	7	200	100
line7	7	8	0.7114	0.2351	6.986	8	200	100
line8	8	9	1.03	0.74	6.986	9	60	20
line9	9	10	1.044	0.74	6.986	10	60	20
line10	10	11	0.1966	0.065	6.986	11	45	30
line11	11	12	0.3744	0.1238	6.986	12	60	35
line12	12	13	1.468	1.155	6.986	13	60	35
line13	13	14	0.5416	0.7129	6.986	14	120	80
line14	14	15	0.591	0.526	6.986	15	60	10
line15	15	16	0.7463	0.545	6.986	16	60	20
line16	16	17	1.289	1.721	6.986	17	60	20
line17	17	18	0.732	0.547	6.986	18	90	40
line18	2	19	0.164	0.1565	6.986	19	90	40
line19	19	20	1.5042	1.3554	6.986	20	90	40
line20	20	21	0.4095	0.4784	6.986	21	90	40
line21	21	22	0.7089	0.9373	6.986	22	90	40
line22	3	23	0.4512	0.3083	6.986	23	90	50
line23	23	24	0.898	0.7091	6.986	24	420	200
line24	24	25	0.896	0.7011	6.986	25	420	200
line25	6	26	0.203	0.1034	6.986	26	60	25
line26	26	27	0.2842	0.1447	6.986	27	60	25
line27	27	28	1.059	0.9337	6.986	28	60	20
line28	28	29	0.8042	0.7006	6.986	29	120	70
line29	29	30	0.5075	0.2585	6.986	30	200	600
line30	30	31	0.9744	0.963	6.986	31	150	70
line31	31	32	0.3105	0.3619	6.986	32	210	100
line32	32	33	0.341	0.5302	6.986	33	60	40
line33	10	34	0.203	0.1034	6.986	34	60	25
line34	34	35	0.2842	0.1447	6.986	35	60	25
line35	35	36	1.059	0.9337	6.986	36	60	20
line36	36	37	0.8042	0.7006	6.986	37	120	70
line37	37	38	0.5075	0.2585	6.986	38	200	600
line38	38	39	0.9744	0.963	6.986	39	150	70
line39	39	40	0.3105	0.3619	6.986	40	210	100
line40	40	41	0.341	0.5302	6.986	41	60	40

Appendix C

Publications

C.1 M.P.S. Pereira, D.Z. Fitiwi, S.F. Santos, J.P.S. Catalão, "Managing RES uncertainty and stability issues in distribution systems via energy storage systems and switchable reactive power sources", in: *Proceedings of the 17th IEEE International Conference on Environment and Electrical Engineering — EEEIC 2017*, Milan, Italy, 6-9 June, 2017

Managing RES Uncertainty and Stability Issues in Distribution Systems via Energy Storage Systems and Switchable Reactive Power Sources

Mário P.S. Pereira[1], D.Z. Fitiwi[2], S.F. Santos[2], J.P.S Catalão[1,2,3]
INESC TEC and FEUP[1], Porto, C-MAST/UBI[2], Covilhã, INESC-ID/IST-UL[3], Lisbon, Portugal
mp0721@gmail.com; dzf@ubi.pt; sdfsantos@gmail.com; catalao@fe.up.pt

***Abstract*—In the last decade, the level of variable renewable energy sources (RESs) integrated in distribution network systems have been continuously growing. This adds more uncertainty to the system, which also faces all traditional sources of uncertainty and those pertaining to other emerging technologies such as demand response and electric vehicles. As a result, distribution system operators are finding it increasingly difficult to maintain an optimal daily operation of such systems. Such challenges/limitations are expected to be alleviated when distribution systems undergo the transformation process to smart grids, equipped with appropriate technologies such as energy storage systems (ESSs) and switchable capacitor banks (SCBs). These technologies offer more flexibility in the system, allowing effective management of the uncertainty in RESs. This paper presents a stochastic mixed integer linear programming (SMILP) model, aiming to optimally operate distribution network systems, featuring variable renewables, and minimizing the impact of RES uncertainty on the system's overall performance via ESSs and SCBs. A standard 41-bus distribution system is employed to show the effectiveness of the proposed S-MILP model. Simulation results indicate that strategically placed ESSs and SCBs can substantially alleviate the negative impact of RES uncertainty in the considered system.**

NOMENCLATURE

A. Sets/Indices

i/Ω^i	Index/set of buses
$g/\Omega^g/\Omega^{DG}$	Index/set of generators/DGs
l/Ω^l	Index/set of branches
s/Ω^s	Index/set of scenarios
h/Ω^h	Index/set of hours
cb/Ω^{cb}	Index/set of capacitor banks
ζ/Ω^{ζ}	Index/set of substations
y	Index of linear segments

B. Parameters

$E^{min}_{es,i}, E^{max}_{es,i}$	Energy storage limits (MWh)
ER_g, ER_{SS}	Emission rates of DGs and energy purchase upstream, respectively (tCO_2e/MWh)
g_l, b_l, S^{max}_l	Conductance, susceptance and flow limit of branch *l*, respectively ($\mho, \mho$ MVA)
$OC_{g,i,s,h}$	Operation cost of DGs (€/MWh)
pf_g	DG power factor
pf_{ss}	Power factor at substation
$Q^{cb,\,max}_i$	Maximum capacitor bank capacity at node *i* (MVAr)
r_l, x_l	Resistance and reactance of branch *l*, respectively (Ω, Ω)
$u_{es,i,h}$	Utilization status of storage system (1 if connected, 0 otherwise)
V_{nom}	Nominal voltage (kV)
$v_{s,h}$	Penalty for unserved power (€/MW)
Y	Total number of linear segments
$\alpha_{l,y}, \beta_{l,y}$	Slopes of linear segments *y* of branch *l*
$\eta^{ch}_{es}, \eta^{dch}_{es}$	Charging and discharging efficiencies of storage systems (%)
$\Delta V^{min}, \Delta V^{max}$	Limits for voltage deviations (kV)
$\lambda^{\zeta}_{s,h}$	Price of electricity purchased from upstream (€/MWh)
$\lambda^{CO2}_{s,h}$	Price of emissions (€/tCO_2e)
ρ_s	Probability of scenario *s*

C. Variables

CET	Total cost of emissions (expected)
COT	Total operation cost (expected)
CUT	Total cost of unserved power (expected)
TC	Total cost (objective function)
$DemP^i_{s,h}$	Active power demand at node *i* (MW)
$DemQ^i_{s,h}$	Reactive power demand at node *i* (MVAr)
$E_{es,i,s,h}$	Stored energy (MWh)
$I^{ch}_{es,i,h}, I^{dch}_{es,i,h}$	Charge and discharge indicator variables, respectively
$P^{SS}_{\zeta,s,h}, Q^{SS}_{\zeta,s,h}$	Active and reactive power import from grid (MW, MVAr)
$P^{ch}_{es,i,s,h}, P^{dch}_{es,i,s,h}$	Charged and discharged power (MW)
$P_{g,i,s,h}$	Active power produced by DGs (MW)
$P^{un}_{i,s,h}, Q^{un}_{i,s,h}$	Active and reactive power unserved at *i* (MW, MVAr)

This work was supported by FEDER funds through COMPETE 2020 and by Portuguese funds through FCT, under Projects SAICT-PAC/0004/2015 - POCI-01-0145-FEDER-016434, POCI-01-0145-FEDER-006961, UID/EEA/50014/2013, UID/CEC/50021/2013, and UID/EMS/00151/2013. Also, the research leading to these results has received funding from the EU Seventh Framework Programme FP7/2007-2013 under grant agreement no. 309048.

978-1-5386-3917-7/17/$31.00 ©

$p_{l,s,h,y}, q_{l,s,h,y}$	Step variables used to linearize the quadratic flows (MW, MVAr)
P_l, Q_l, θ_l	Active and reactive power flows, and voltage angle difference of branch *l*, respectively (MW, MVAr, radians)
$PL_{l,s,h}, QL_{l,s,h}$	Active and reactive power losses of branch *l* (MW, MVAr)
$Q_{g,i,s,h}$	Active power produced/consumed by DGs (MVAr)
$Q^{cb}_{i,s,h}$	Reactive power injected at node *i* by capacitor bank (MVAr)
$V_{i,s,h}, V_{j,s,h}$	Voltage magnitudes of node *i* and *j* within the same branch (kV)
$\theta_{i,s,h}, \theta_{j,s,h}$	Voltage angles at node *i* and *j* within the same branch (radians)
$\lambda^{dch}_{s,h}$	Cost of storage system (€/MWh)

I. Introduction

Power systems have experienced significant changes in the last decade. In particular, distribution network systems are now gradually evolving from passive to active network systems. These changes are as a result of the need for the energy systems to adapt to new challenges such as the continuous increase in demand for electricity [1], environmental concerns associated with conventional power generation practices, energy transmission and distribution, etc. In order to partly overcome such challenges, distributed generation (DG) systems (renewables, in particular) have been integrated in the energy systems, which is becoming a common practice throught the world.

However, the integration of variable renewable energy sources (RESs) comes with several challenges, both economic and technical. On the technical side, the first major challenge that immediately comes with RES integration is related to the uncertainty and variability of renewables, which "make the management of network systems very difficult" [2]. Furthermore, violations of system-wide technical restrictions are not tolerated especially at distribution levels, that is, the system should always operate respecting the technical limitations [3]. On the economical point of view, the non-dispatchable nature of RES, especially wind and solar, brings additional costs. To overcome these challenges several countries are investing in planning and expanding their current infrastructure to cope with RES integration [4]. It is necessary to introduce technologies that facilitate the integration of variable RESs and their effective management. Among others, the optimal use of energy storage systems (ESSs) and switchable capacitor banks (SCBs) is a viable option capable of addressing the aforementioned challenges, at least partly.

It is now widely accepted that ESSs will be extremely important components of future power systems because they help to counteract the unpredictable variation of the energy generated using RESs, as well as the uncertainty associated with power supply, which adversely affects the optimal operation and reliability of the traditional electrical systems [5]. Therefore, the use of ESSs allows to level the incompatibility between energy generation and demand [6], [7]. In addition, ESSs can contribute to relieving the fluctuation of power from RESs, low voltage ride through, and voltage support, resulting in smoother system operations. In [8], the wide-range benefits of using ESSs in the distribution system are extensively discussed. Despite all this, ESSs are yet very expensive. However, with the continuous technological development, the cost of most ESS technologies has been decreasing with high learning rates. A recent study on cost-benefit analysis of ESSs has shown that ESSs are becoming increasingly competitive, and the use of such technologies is justified in many cases [8].

Another relatively cheaper technology that allows greater integration and management of RESs is switchable capacitor bank. This is due to the fact that power systems require a significant amount of reactive power to maintain the voltage in the nodes within specified ranges. There are several switching methods such as the VAR compensation source but the most commonly used is switchable capacitor banks since capacitors are passive filters and do not interfere with the optimization process [9]. Therefore, capacitor banks are widely used as effective technologies, both at the transmission and distribution levels. In addition to maintaining the nodal voltages at standard levels, capacitor banks can be used to reduce energy losses by injecting reactive power into substations [10], thereby increasing system capacity and correcting system power factor [11]. Capacitor banks placement along the line will compensate for the inductive or reactance's loads of the lines [12]. In the literature, several capacitor bank positioning techniques have been proposed as in [10], [13]–[15].

This work develops a new stochastic MILP model that aims to ensure a more efficient utilization of variable renewables at distribution levels. In addition, the model is used for managing the uncertainty inherent to such energy sources with properly located ESSs and SCBs, thereby maintaining the stability and the integrity of distribution networks systems as well as the power quality in the system.

II. Mathematical Formulation

A. Objective Function

As described in [16], the location of the different resources is already predetermined. The objective of this work is to investigate an optimal operation of distribution grids featuring large-scale RES based DGs, SCBs and ESSs, in order to cope with the variability of wind and solar power production.

The objective function minimizes the sum of expected costs of operation, emission, unserved energy and emissions along the optimization scope.

$$MinTC = COT + CUT + CET \tag{1}$$

The total operation cost is given by the sum of expected costs of power generation by DGs, import power and discharged power as:

$$
\begin{aligned}
COT = & \sum_{s\in\Omega^s} \rho_s * \sum_{h\in\Omega^h} \sum_{g\in\Omega^g} \sum_{i\in\Omega^i} OC_{g,i,s,h} * P_{g,i,s,h} \\
& + \sum_{s\in\Omega^s} \rho_s * \sum_{h\in\Omega^h} \sum_{\zeta\in\Omega^\zeta} \lambda^{\zeta}_{s,h} * P^{SS}_{\zeta,s,h} \\
& + \sum_{s\in\Omega^s} \rho_s * \sum_{h\in\Omega^h} \sum_{es\in\Omega^{es}} \sum_{i\in\Omega^i} \lambda^{dch}_{s,h} * P^{dch}_{es,i,s,h}
\end{aligned} \tag{2}
$$

Cost of discharge is considered to account for the degradation of the energy storage system.

To model the total cost of unserved power cost, a penalty ($v_{s,h}$) is considered:

$$
CUT = \sum_{s\in\Omega^s} \rho_s * \sum_{h\in\Omega^h} \sum_{i\in\Omega^i} v_{s,h} * (P^{un}_{i,s,h} + Q^{un}_{i,s,h}) \tag{3}
$$

The final equation that is part of the objective function refers to the total cost of emissions. It is modeled as:

$$
\begin{aligned}
CET = & \sum_{s\in\Omega^s} \rho_s * \sum_{h\in\Omega^h} \sum_{g\in\Omega^g} \sum_{i\in\Omega^i} \lambda^{CO2}_{s,h} * ER_g * P_{g,i,s,h} \\
& + \sum_{s\in\Omega^s} \rho_s * \sum_{h\in\Omega^h} \sum_{\zeta\in\Omega^\zeta} \lambda^{CO2}_{s,h} * ER_{SS} * P^{SS}_{\zeta,s,h}
\end{aligned} \tag{4}
$$

B. Constraints

For computation reasons, the non-linear and non-convex AC power flow equations are often linearized under various simplifying assumptions. Here, the linearized AC network model proposed in [17] is being considered. The linearized active and reactive power flow constraints are:

$$
P_{l,s,h} \approx V_{nom}(\Delta V_{i,s,h} - \Delta V_{j,s,h}) g_l - V^2_{nom} b_l(\theta_{l,s,h}) \tag{5}
$$

$$
Q_{l,s,h} \approx -V_{nom}(\Delta V_{i,s,h} - \Delta V_{j,s,h}) b_l - V^2_{nom} g_l(\theta_{l,s,h}) \tag{6}
$$

The thermal limit in a feeder is given by:

$$
P^2_{l,s,h} + Q^2_{l,s,h} \leq (S^{max}_l)^2 \tag{7}
$$

The quadratic expression (7) is linearized using a piecewise linearization, considering a sufficient number of linear segments, *Y*. In this study, *Y* is considered equal to 5, a number which balances accuracy with computation burden [18]. There are several ways of linearizing such functions as described in [19]. This approach is based on a first-order approximation of a non-linear curve, and is chosen due to its relatively simple formulation. In order to reduce the mathematical complexity of the formulation, two non-negative auxiliary variables are introduced for each of the flows P_l and Q_l, where $P_l = P^+_l - P^-_l$ and $Q_l = Q^+_l - Q^-_l$. These auxiliary variables (P^+_l, P^-_l, Q^+_l and Q^-_l) represent the positive and negative flows of P_l and Q_l, respectively.

The associated constraints, in this case, are presented below:

$$
P^2_{l,s,h} \approx \sum_{y=1}^{Y} \alpha_{l,y} p_{l,s,h,y} \tag{8}
$$

$$
Q^2_{l,s,h} \approx \sum_{y=1}^{Y} \beta_{l,y} q_{l,s,h,y} \tag{9}
$$

$$
P^+_{l,s,h} + P^-_{l,s,h} = \sum_{y=1}^{Y} p_{l,s,h,y} \tag{10}
$$

$$
Q^+_{l,s,h} + Q^-_{l,s,h} = \sum_{y=1}^{Y} q_{l,s,h,y} \tag{11}
$$

where $p_{l,s,h,y} \leq S^{max}_l / Y$ and $q_{l,s,h,y} \leq S^{max}_l / Y$.

The active and reactive power losses in line l can be approximated as:

$$
PL_{l,s,h} = r_l (P^2_{l,s,h} + Q^2_{l,s,h}) / V^2_{nom} \tag{12}
$$

$$
QL_{l,s,h} = x_l (P^2_{l,s,h} + Q^2_{l,s,h}) / V^2_{nom} \tag{13}
$$

The details related to (12) and (13) can be found in [17].

To ensure that, at all time, load balances are respected, the sum of of all injections should be equal to the sum of all withdrawals at each node for both active (14) and reactive (15) loads, which is *Kirchhoff's Current Law*:

$$
\begin{aligned}
& P^{SS}_{\zeta,s,h} + \sum_{g\in\Omega^{DG}} P_{g,i,s,h} + \sum_{es\in\Omega^{es}} (P^{dch}_{es,i,s,h} - P^{ch}_{es,i,s,h}) \\
& + \sum_{in,l\in i} P_{l,s,h} - \sum_{out,l\in i} P_{l,s,h} + P^{un}_{i,s,h} \\
& = Dem P^i_{s,h} + \sum_{in,l\in i} \frac{1}{2} PL_{l,s,h} + \sum_{out,l\in i} \frac{1}{2} PL_{l,s,h} \; \forall\, \zeta \in i
\end{aligned} \tag{14}
$$

$$
\begin{aligned}
& Q^{SS}_{\zeta,s,h} + \sum_{g\in\Omega^{DG}} Q_{g,i,s,h} + \sum_{cb\in\Omega^{cb}} Q^{cb}_{i,s,h} \\
& + \sum_{in,l\in i} Q_{l,s,h} - \sum_{out,l\in i} Q_{l,s,h} \\
& = Dem Q^i_{s,h} + \sum_{in,l\in i} \frac{1}{2} QL_{l,s,h} + \sum_{out,l\in i} \frac{1}{2} QL_{l,s,h} \; \forall\, \zeta \in i
\end{aligned} \tag{15}
$$

ESS constraints are presented below:

$$
0 \leq P^{ch}_{es,i,s,h} \leq u_{es,i,h} I^{ch}_{es,i,h} P^{ch,max}_{es,i,s,h} \tag{16}
$$

$$
0 \leq P^{dch}_{es,i,s,h} \leq u_{es,i,h} I^{dch}_{es,i,h} P^{dch,max}_{es,i,s,h} \tag{17}
$$

$$
I^{ch}_{es,i,h} + I^{ch}_{es,i,h} \leq 1 \tag{18}
$$

$$
\begin{aligned}
E_{es,i,s,h} = & E_{es,i,s,h-1} + \eta^{ch}_{es} P^{ch}_{es,i,s,h} \\
& - \beta^{dch}_{es} P^{dch}_{es,i,s,h} \text{ where } \beta^{dch}_{es} = \frac{1}{\eta^{dch}_{es}}
\end{aligned} \tag{19}
$$

$$
E^{min}_{es,i,s,h} u_{es,i,h} \leq E_{es,i,s,h} \leq E^{max}_{es,i,s,h} u_{es,i,h} \tag{20}
$$

$$
E_{es,i,s,h_0} = \mu_{es} u_{es,i,h} E^{max}_{es,i} \tag{21}
$$

$$
E_{es,i,s,h_f} = E_{es,i,s,h_0} \tag{22}
$$

The charging and discharging limits related to ESS are depicted in (16) and (17), respectively. Note that $u_{es,i,h}$ is a control variable, set to 1 in this study, that defines if a storage unit is connected or not. Constraint (18) ensures that charging and discharging cannot occur simultaneously. The amount of energy available in ESS at hour *h* depends on the state of charge at the previous hour and on the charge or discharge cycle, on hour *h*, as demonstrated in (19). The maximum and

minimum storage capacity at hour *h* are also considered in (20). Constraints (21) and (22) ensure that there is an initial charge storage level (21), and that at the end of the cycle (h_f) the amount of energy stored is the same as the initial ESS level (22). These constraints ensure that the obtained solution does not depend on the initial reservoir level.

Charging and discharging inefficiencies are considered in order to model losses (electrical, chemical, etc.). In this study, charging and discharging efficiencies are considered equal.

Active and reactive power limits related to DGs are presented below:

$$0 \leq P_{g,i,s,h} \leq P^{max}_{g,i,s,h} \tag{23}$$

$$0 \leq Q_{g,i,s,h} \leq Q^{max}_{g,i,s,h} \tag{24}$$

In the case of variable generation sources, $P^{max}_{g,i,s,h}$ should be equal to the actual production at a specific hour. In this study, wind and solar (PV) type DGs are considered to have reactive power support capabilities. To model this, the following constraint must be considered:

$$-\tan(\cos^{-1}(pf_g)) * P_{g,i,s,h} \leq Q_{g,i,s,h} \tag{25}$$

$$Q_{g,i,s,h} \leq \tan(\cos^{-1}(pf_g)) * P_{g,i,s,h} \tag{26}$$

In (25) and (26) it can be observed that, DGs are capable of operating between a leading and lagging power factor.

The reactive power at the substation is constrained as:

$$Q^{SS,\,min}_{\zeta,s,h} \leq Q^{SS}_{\zeta,s,h} \leq Q^{SS,\,max}_{\zeta,s,h} \tag{27}$$

where the minimum and maximum reactive power limits could be calculated as in (28) and (29):

$$Q^{SS,\,max}_{\zeta,s,h} = \tan(\cos^{-1}(pf_{ss})) * P^{SS}_{\zeta,s,h} \tag{28}$$

$$Q^{SS,\,min}_{\zeta,s,h} = -\tan(\cos^{-1}(pf_{ss})) * P^{SS}_{\zeta,s,h} \tag{29}$$

The following constraint related to capacitor banks ensures the reactive power produced is bounded between zero and the maximum capacity:

$$0 \leq Q^{cb}_{i,s,h} \leq Q^{cb,\,max}_{i} \tag{30}$$

III. Case Study, Results and Discussion

A. System Data and Assumptions

Information regarding the radial network used to test the proposed operation model, can be found in [16]. For the base case, no lower voltage restrictions were considered, and the presented results correspond to a substation power factor of 0.8. This power factor, despite unrealistic, was chosen to ensure that, on the base case, all of the reactive demand was met. Note that for the base case, all DGs, SCBs and ESSs are not connected. This way, the only available power comes from the upstream grid, which would mean that there would be unserved reactive demand for high power factors. To ease the analysis of different cases and scenarios, the minimum power factor at the substation level was maintained at 0.8.

The location of capacitor banks, energy storage systems and DGs can also be found in [16], with the only change on the installed wind capacity on bus 14 which is now 2 MW instead of 3 MW. This change was made in order to better evaluate the impact of ESS in coping with the variability of RES. In this study, as mentioned in II-B, DGs are considered to have a reactive power support with a power factor of 0.95.

In addition, the following assumptions were made when carrying out the simulations:

- A 24 hour period was considered.
- Electricity price follows the same trend as demand.
- Nominal voltage is 12.66 kV.
- $\Delta V^{min} = -5\% * V_{nom}$ and $\Delta V^{max} = 5\% * V_{nom}$.
- The number of partitions (*Y*) is set equal to 5.
- $\eta^{ch}_{es} = 90\%$, unless otherwise mentioned.
- $ER_{SS} = 0.4\ tCO_2e/MWh$.
- Emission rate of DGs is set to 0.0276 and 0.0584 tCO_2e/MWh for wind and solar, respectively.
- $\lambda^{CO2}_{s,h} = 6$ €/tCO_2e.
- Electricity tariffs of wind and solar power generators are 20 and 40 €/MWh, respectively.
- $\lambda^{dch}_{s,h} = 5$ €/MWh.
- At node 1, $V_1 = V_{nom}$ and $\theta_1 = 0$.
- $v_{s,h} = 3000$ €/MW.

This study considers the combination of ten different scenarios for representing uncertainty related to demand, wind and solar power outputs, leading to a total of 1000 scenarios.

B. Results and Discussions

In order to analyze the behavior and impact of DGs, ESS and SCBs on the system, several cases were considered:

- Base case: Only importing power from the upstream grid is considered, while DGs, ESSs and SCBs are not connected.
- CB only: Only SCBs are connected, while DGs and ESSs are not.
- Efficiency (EFF) 0.9: DGs, ESSs and SCBs are connected. Storage efficiency set to 90%.
- EFF 0.8: The same as case "EFF 0.9", but ESS efficiency was reduced to 80%.
- EFF 0.7: The same as case "EFF 0.9", but ESS efficiency was reduced to 70%.
- Lim Q: The same as case "EFF 0.9", but constraints related to reactive power were not considered.

For each case, other than the "Lim Q" one, reactive power constraints were considered. The purpose of removing these constraints for the last case was to observe the behavior of the system when power export was allowed.

Voltage profiles for all cases can be seen in Fig. 1. It can be observed that for the base case, voltage deviations surpassed the minimum limit due to the high reactive power requirement in the system. To avoid infeasibility, in addition to lowering the power factor of the substation to 0.8, there was a need to remove the minimum voltage deviation constraints, only for the base case.

Emissions and import costs for each case, as well as the corresponding average losses are presented in Table I.

As expected, for the base case, where only import is considered, voltage deviations increased throughout the system

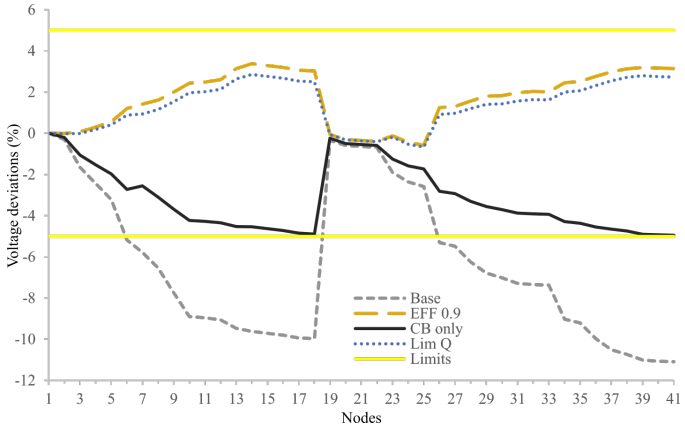

Fig. 1. Average voltage deviations at each node for each case

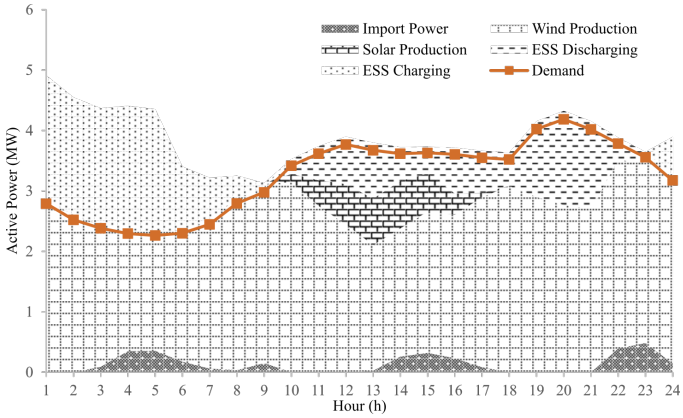

Fig. 2. Energy mix for Case: EFF 0.9

TABLE I
RELEVANT SYSTEM VARIABLES FOR EACH CASE

Case	Base	CB only	EFF 0.9	EFF 0.8	EFF 0.7	Lim Q
Operation Cost (€)						
DG	0	0	1667.83	1699.13	1724.28	1788.28
ESS	0	0	52.84	43.25	29.08	67.87
Cost of Import (€)	5999.8	5842.75	180.65	267.27	364.29	-214.14
Cost of Emissions (€)						
DG	0	0	13.88	14.15	14.38	14.92
Substation	205.87	200.34	7.67	10.33	12.62	2.66
Total Cost (€)	6205.67	6043.09	1922.87	2034.13	2144.65	1659.58
Average Losses						
PL (MW)	0.33	0.23	0.1	0.09	0.09	0.15
QL (MVAr)	0.23	0.17	0.08	0.08	0.07	0.11

especially for buses on the far end. Furthermore, as bus 1 is considered to have a deviation of 0%, then all downstream buses will have a negative voltage deviation, as power flows from upstream to downstream, a classic system power flow. Note that profiles shown above represent averages. The voltage deviation, for the base case, at bus 41 could vary between -7.7% and -14.3% for low and high demand scenarios, respectively. In the matter of cost in this case, there is a high cost of imported energy and the respective emission cost. Moreover, this case presents the highest value of both active and reactive power losses.

With the inclusion of capacitor banks (Case CB only), voltage deviation could be managed since there are now reactive power sources within the system. Voltage profiles now respect the limits as it can be seen in Fig. 1. By including capacitor banks, losses have decreased (Table I), as expected, which in turn affected the imported power, reducing the amount of both active and reactive power required from the substation. Including reactive power sources reduced cost by 2.6%, and more importantly, voltage deviations improved on average by 45.1% respecting the imposed limits. Since in this case only the upstream grid and SCBs were considered, costs only concern imported power and its respective emissions, as in the first case. In addition, this case also follows the classic grid active power flow.

Considering all technologies connected to the grid (DGs, ESSs and SCBs) there is a complete change on the voltage profile, as seen in Fig. 1, for all remaining cases. As DGs were included, voltage profiles were altered so that power flows can now occur from downstream to upstream. For example, bus 14, 32 and 38 have the highest installed capacity of DGs, and each one of these buses belongs to a different branch of the grid, and are located near the end of the corresponding branch. As it can be observed in Fig. 1, bus 14 and 32 have the highest positive deviation (of the corresponding branch), which means they dispatch energy for the surrounding buses and loads, because production surpasses the local demand. As for bus 38, it has another bus with DGs in the same branch (bus 39), it dispatches power to upstream buses since demand at node 39, 40 and 41 are met by the local production at bus 39. Note that the situation at bus 38 only occurs because local production at bus 39 surpasses local demand.

The energy mix for the case where DGs, ESSs and SCBs are connected to the system can be analyzed in Fig. 2. It can be observed that during valley hours, the system uses the excess wind power production and a slight import of power, since prices are low, to charge the energy storage systems. When wind power production diminishes, ESSs begin to discharge and together with solar production the demand is met. Because solar power production is more expensive, regarding tariffs, than ESSs and wind power production, we observed a curtailment of solar power since discharging the stored energy was cheaper, because it originated from wind type DGs. Despite being more expensive, solar PVs must be used, since later in the day, there will not be any and power import will be more expensive. In other words, a total curtailment of solar power would be counterproductive since ESSs can be used more efficiently later in the day, and also because it would mean curtailing a valuable resource totally dependent on the time of day. In order to compensate the lack of solar power during peak hours, when electricity prices are higher, ESSs can be used to partially meet demand, avoiding the need to import energy at high prices.

The difference in the actual power production and demand profiles (visible during peak hours) is because of losses in the system.

Considering ESSs with lower efficiencies leads to a decrease in the utilization of these systems, since it would require more energy to use them efficiently. When ESS efficiency is reduced, the otherwise curtailed solar production must now be used to compensate. In Table I, both cases with altered efficiencies presented a higher cost of operation and emissions of DGs, because of increased use of solar power, and at the same time more import power cost, and respective emissions, since stored energy was intended to be used later in the day when electricity price is higher. On the other hand, losses decreased slightly when compared to Case: EFF 0.9 since less discharge power was used. Moreover, voltage profiles did not change significantly for different ESS efficiencies (i.e cases EFF 0.8 and EFF 0.7) when compared to the profile in case EFF 0.9.

When excluding the reactive power limits, export is now allowed, which means import prices can be negative (excess power can be sold to the grid), reducing the objective function. This is proved by the fact that this case presents the lowest cost, as demonstrated in Table I. Losses increase because DG nodes are on the far end of the grid and in order to export active power, it must pass through several lines until it reaches the substation, increasing losses (when compared with Case: EFF 0.9). However, they are still less than in the Base case. Voltage profiles are slightly improved when compared to EFF 0.9 case, since there is active power export at the same time as reactive power import.

IV. Conclusion

This work proposed a new stochastic MILP model that aims to ensure a more efficient utilization of variable renewables at distribution levels. The results show that the integration of ESS together with reactive power sources could cope with the variability of RES, reducing losses and cost, while improving voltage profiles.

Because of ESS, renewable energy penetration increased significantly, since excess wind power could be stored and used later, instead of being curtailed. This way, the integration of ESS allows a more efficient use of renewable energy sources, which are almost emission-free power source, and this is reflected in the cost. In fact, RESs can represent 96% of the total power production. A good planning of the location and capacity of RES is also required, since this will affect losses and depending on the locations, sizes as well as the profile of wind and solar outputs. As demonstrated in this study, with the integration of RESs, ESSs and SCBs in the right locations, active power losses in the EFF 0.9 case could be reduced by 70% on average, and total cost in the same case by 69%. Furthermore, the proposed model considerably improves voltage profiles in the system, which in turn contributes to an increased voltage stability margin which is essential for a secure operation of the system.

References

[1] B. Muruganantham, R. Gnanadass, and N. Padhy, "Challenges with renewable energy sources and storage in practical distribution systems," Renewable and Sustainable Energy Reviews, vol. 73, pp. 125–134, June 2017.

[2] S. Nandi, P. Biswas, V. N. Nandakumar, and R. K. Hedge, "Two novel schemes suitable for static switching of three-phase delta-connected capacitor banks with minimum surge current," IEEE Transactions on Industry Applications, vol. 33, no. 5, pp. 1348–1354, 1997.

[3] H. Nosair and F. Bouffard, "Flexibility Envelopes for Power System Operational Planning," IEEE Transactions on Sustainable Energy, vol. 6, pp. 800–809, July 2015.

[4] W. A. Bukhsh, C. Zhang, and P. Pinson, "An Integrated Multiperiod OPF Model With Demand Response and Renewable Generation Uncertainty," IEEE Transactions on Smart Grid, vol. 7, pp. 1495–1503, May 2016.

[5] M. Masoum, A. Jafarian, M. Ladjevardi, E. Fuchs, and W. Grady, "Fuzzy Approach for Optimal Placement and Sizing of Capacitor Banks in the Presence of Harmonics," IEEE Transactions on Power Delivery, vol. 19, pp. 822–829, Apr. 2004.

[6] B. Zakeri and S. Syri, "Electrical energy storage systems: A comparative life cycle cost analysis," Renewable and Sustainable Energy Reviews, vol. 42, pp. 569–596, Feb. 2015.

[7] A. Colmenar-Santos, C. Reino-Rio, D. Borge-Diez, and E. Collado-Fernández, "Distributed generation: A review of factors that can contribute most to achieve a scenario of DG units embedded in the new distribution networks," Renewable and Sustainable Energy Reviews, vol. 59, pp. 1130–1148, June 2016.

[8] P. Poonpun and W. Jewell, "Analysis of the Cost per Kilowatt Hour to Store Electricity," IEEE Transactions on Energy Conversion, vol. 23, pp. 529–534, June 2008.

[9] M. H. Tushar and C. Assi, "Volt-VAR Control through Joint Optimization of Capacitor Bank Switching, Renewable Energy, and Home Appliances," IEEE Transactions on Smart Grid, pp. 1–1, 2017.

[10] S. Soto and V. Hinojosa, "Stochastic optimal allocation of reactive power banks for system loss minimization," IEEE Latin America Transactions, vol. 14, no. 4, pp. 1980–1987, 2016.

[11] K. Hur and S. Santoso, "Distance Estimation of Switched Capacitor Banks in Utility Distribution Feeders," IEEE Transactions on Power Delivery, vol. 22, pp. 2419–2427, Oct. 2007.

[12] S. Santoso, "On Determining the Relative Location of Switched Capacitor Banks," IEEE Transactions on Power Delivery, vol. 22, pp. 1108–1116, Apr. 2007.

[13] R. Jabr, "Optimal placement of capacitors in a radial network using conic and mixed integer linear programming," Electric Power Systems Research, vol. 78, pp. 941–948, June 2008.

[14] S. Segura, R. Romero, and M. J. Rider, "Efficient heuristic algorithm used for optimal capacitor placement in distribution systems," International Journal of Electrical Power & Energy Systems, vol. 32, pp. 71–78, Jan. 2010.

[15] H. Khani, M. Moallem, S. Sadri, and M. Dolatshahi, "A New Method for Online Determination of the Location of Switched Capacitor Banks in Distribution Systems," IEEE Transactions on Power Delivery, vol. 26, pp. 341–351, Jan. 2011.

[16] S. F. Santos, D. Z. Fitiwi, M. Shafie-khah, A. W. Bizuayehu, C. M. P. Cabrita, and J. P. S. Catalao, "New multi-stage and stochastic mathematical model for maximizing RES hosting capacity—part II: Numerical results," vol. 8, no. 1, pp. 320–330.

[17] S. F. Santos, D. Z. Fitiwi, M. Shafie-Khah, A. W. Bizuayehu, C. M. P. Cabrita, and J. P. S. Catalao, "New multistage and stochastic mathematical model for maximizing RES hosting capacity—part I: Problem formulation," vol. 8, no. 1, pp. 304–319.

[18] D. Z. Fitiwi, L. Olmos, M. Rivier, F. de Cuadra, and I. Pérez-Arriaga, "Finding a representative network losses model for large-scale transmission expansion planning with renewable energy sources," vol. 101, pp. 343–358.

[19] J. P. Vielma, S. Ahmed, and G. Nemhauser, "Mixed-Integer Models for Nonseparable Piecewise-Linear Optimization: Unifying Framework and Extensions," Operations Research, vol. 58, pp. 303–315, Apr. 2010.

References

[1] M. Nicolini and M. Tavoni, "Are renewable energy subsidies effective? Evidence from Europe," *Renewable and Sustainable Energy Reviews*, vol. 74, pp. 412–423, July 2017.

[2] K. P. Kumar and B. Saravanan, "Recent techniques to model uncertainties in power generation from renewable energy sources and loads in microgrids – A review," *Renewable and Sustainable Energy Reviews*, vol. 71, pp. 348–358, May 2017.

[3] P. Paliwal, N. Patidar, and R. Nema, "Planning of grid integrated distributed generators: A review of technology, objectives and techniques," *Renewable and Sustainable Energy Reviews*, vol. 40, pp. 557–570, Dec. 2014.

[4] B. R. Pereira, G. R. M. Martins da Costa, J. Contreras, and J. R. S. Mantovani, "Optimal Distributed Generation and Reactive Power Allocation in Electrical Distribution Systems," *IEEE Transactions on Sustainable Energy*, vol. 7, pp. 975–984, July 2016.

[5] O. Homaee, A. Zakariazadeh, and S. Jadid, "Real-time voltage control algorithm with switched capacitors in smart distribution system in presence of renewable generations," *International Journal of Electrical Power & Energy Systems*, vol. 54, pp. 187–197, Jan. 2014.

[6] "Electricity and heat statistics." http://ec.europa.eu/eurostat/statistics-explained/index.php/Electricity_and_heat_statistics#Production_of_electricity. [Accessed: 11-May-2017].

[7] "Energy from renewable sources." http://ec.europa.eu/eurostat/statistics-explained/index.php/Energy_from_renewable_sources. [Accessed: 14-May-2017].

[8] T. D. Corsatea, S. Giaccaria, C.-F. Covrig, N. Zaccarelli, and M. Ardelean, "RES diffusion and R&D investments in the flexibilisation of the European electricity networks," *Renewable and Sustainable Energy Reviews*, vol. 55, pp. 1069–1082, Mar. 2016.

[9] W.-S. Tan, M. Y. Hassan, M. S. Majid, and H. Abdul Rahman, "Optimal distributed renewable generation planning: A review of different approaches," *Renewable and Sustainable Energy Reviews*, vol. 18, pp. 626–645, Feb. 2013.

[10] W. A. Bukhsh, C. Zhang, and P. Pinson, "An Integrated Multiperiod OPF Model With Demand Response and Renewable Generation Uncertainty," *IEEE Transactions on Smart Grid*, vol. 7, pp. 1495–1503, May 2016.

[11] B. Muruganantham, R. Gnanadass, and N. Padhy, "Challenges with renewable energy sources and storage in practical distribution systems," *Renewable and Sustainable Energy Reviews*, vol. 73, pp. 125–134, June 2017.

[12] M. Katsanevakis, R. A. Stewart, and J. Lu, "Aggregated applications and benefits of energy storage systems with application-specific control methods: A review," *Renewable and Sustainable Energy Reviews*, vol. 75, pp. 719–741, Aug. 2017.

[13] M. S. Guney and Y. Tepe, "Classification and assessment of energy storage systems," *Renewable and Sustainable Energy Reviews*, vol. 75, pp. 1187–1197, Aug. 2017.

[14] L. H. Macedo, J. F. Franco, M. J. Rider, and R. Romero, "Optimal Operation of Distribution Networks Considering Energy Storage Devices," *IEEE Transactions on Smart Grid*, vol. 6, pp. 2825–2836, Nov. 2015.

[15] N. Jayasekara, M. A. S. Masoum, and P. J. Wolfs, "Optimal Operation of Distributed Energy Storage Systems to Improve Distribution Network Load and Generation Hosting Capability," *IEEE Transactions on Sustainable Energy*, vol. 7, pp. 250–261, Jan. 2016.

[16] C. A. Silva-Monroy and J.-P. Watson, "Integrating Energy Storage Devices Into Market Management Systems," *Proceedings of the IEEE*, vol. 102, pp. 1084–1093, July 2014.

[17] M. Masoum, A. Jafarian, M. Ladjevardi, E. Fuchs, and W. Grady, "Fuzzy Approach for Optimal Placement and Sizing of Capacitor Banks in the Presence of Harmonics," *IEEE Transactions on Power Delivery*, vol. 19, pp. 822–829, Apr. 2004.

[18] B. Zakeri and S. Syri, "Electrical energy storage systems: A comparative life cycle cost analysis," *Renewable and Sustainable Energy Reviews*, vol. 42, pp. 569–596, Feb. 2015.

[19] A. Colmenar-Santos, C. Reino-Rio, D. Borge-Diez, and E. Collado-Fernández, "Distributed generation: A review of factors that can contribute most to achieve a scenario of DG units embedded in the new distribution networks," *Renewable and Sustainable Energy Reviews*, vol. 59, pp. 1130–1148, June 2016.

[20] P. Poonpun and W. Jewell, "Analysis of the Cost per Kilowatt Hour to Store Electricity," *IEEE Transactions on Energy Conversion*, vol. 23, pp. 529–534, June 2008.

[21] M. H. Tushar and C. Assi, "Volt-VAR Control through Joint Optimization of Capacitor Bank Switching, Renewable Energy, and Home Appliances," *IEEE Transactions on Smart Grid*, pp. 1–1, 2017.

[22] S. Soto and V. Hinojosa, "Stochastic optimal allocation of reactive power banks for system loss minimization," *IEEE Latin America Transactions*, vol. 14, no. 4, pp. 1980–1987, 2016.

[23] R. Jabr, "Optimal placement of capacitors in a radial network using conic and mixed integer linear programming," *Electric Power Systems Research*, vol. 78, pp. 941–948, June 2008.

[24] S. Segura, R. Romero, and M. J. Rider, "Efficient heuristic algorithm used for optimal capacitor placement in distribution systems," *International Journal of Electrical Power & Energy Systems*, vol. 32, pp. 71–78, Jan. 2010.

[25] A. Ameli, A. Ahmadifar, M.-H. Shariatkhah, M. Vakilian, and M.-R. Haghifam, "A dynamic method for feeder reconfiguration and capacitor switching in smart distribution systems," *International Journal of Electrical Power & Energy Systems*, vol. 85, pp. 200–211, Feb. 2017.

[26] K. Hur and S. Santoso, "Distance Estimation of Switched Capacitor Banks in Utility Distribution Feeders," *IEEE Transactions on Power Delivery*, vol. 22, pp. 2419–2427, Oct. 2007.

[27] S. Santoso, "On Determining the Relative Location of Switched Capacitor Banks," *IEEE Transactions on Power Delivery*, vol. 22, pp. 1108–1116, Apr. 2007.

[28] S. Nandi, P. Biswas, V. N. Nandakumar, and R. K. Hedge, "Two novel schemes suitable for static switching of three-phase delta-connected capacitor banks with minimum surge current," *IEEE Transactions on Industry Applications*, vol. 33, no. 5, pp. 1348–1354, 1997.

[29] H. Nosair and F. Bouffard, "Flexibility Envelopes for Power System Operational Planning," *IEEE Transactions on Sustainable Energy*, vol. 6, pp. 800–809, July 2015.

[30] S. F. Santos, D. Z. Fitiwi, M. Shafie-Khah, A. W. Bizuayehu, C. M. P. Cabrita, and J. P. S. Catalao, "New Multistage and Stochastic Mathematical Model for Maximizing RES Hosting Capacity—Part I: Problem Formulation," *IEEE Transactions on Sustainable Energy*, vol. 8, pp. 304–319, Jan. 2017.

[31] D. Z. Fitiwi, L. Olmos, M. Rivier, F. de Cuadra, and I. Pérez-Arriaga, "Finding a representative network losses model for large-scale transmission expansion planning with renewable energy sources," *Energy*, vol. 101, pp. 343–358, Apr. 2016.

[32] J. P. Vielma, S. Ahmed, and G. Nemhauser, "Mixed-Integer Models for Nonseparable Piecewise-Linear Optimization: Unifying Framework and Extensions," *Operations Research*, vol. 58, pp. 303–315, Apr. 2010.

[33] S. F. Santos, D. Z. Fitiwi, M. Shafie-khah, A. W. Bizuayehu, C. M. P. Cabrita, and J. P. S. Catalao, "New Multi-Stage and Stochastic Mathematical Model for Maximizing RES Hosting Capacity—Part II: Numerical Results," *IEEE Transactions on Sustainable Energy*, vol. 8, pp. 320–330, Jan. 2017.

[34] T. Lambert, P. Gilman, and P. Lilienthal, "Micropower system modeling with HOMER," *Integration of alternative sources of energy*, vol. 1, no. 15, pp. 379–418, 2006.

[35] Y. Li, Q. Wu, M. Li, and J. Zhan, "Mean-variance model for power system economic dispatch with wind power integrated," *Energy*, vol. 72, pp. 510–520, Aug. 2014.

[36] M. Zhao, Z. Chen, and F. Blaabjerg, "Probabilistic capacity of a grid connected wind farm based on optimization method," *Renewable Energy*, vol. 31, pp. 2171–2187, Oct. 2006.

[37] M. Aien, M. Rashidinejad, and M. Fotuhi-Firuzabad, "On possibilistic and probabilistic uncertainty assessment of power flow problem: A review and a new approach," *Renewable and Sustainable Energy Reviews*, vol. 37, pp. 883–895, Sept. 2014.